6 Variability and Noise in Nets of Hodgkin-Huxley Elements

The Hodgkin-Huxley (HH) model [31] is, as stated in Chapter 2, a standard model to describe neuronal dynamics. Many studies deal with the influence of noise on this model. It was shown, for instance, that additive noise may lead to stochastic resonance [66] and coherence resonance [67] in a single HH element. Furthermore resonance effects and synchronisation under the influence of noise have been studied in globally coupled nets of HH elements [68].

In this chapter the influence of variability and noise on nets of Hodgkin-Huxley elements [Eqs. (3.12)] and nets of reduced Hodgkin-Huxley elements [Eqs. (3.14)] with global [Eq. (2.16)] and diffusive [Eq. (2.18)] coupling is studied in detail. In the first part of Section 6.1 the interplay of additive variability and additive noise is studied in oscillatory nets. Furthermore, in the second part of this section, oscillatory nets under the influence of multiplicative variability and multiplicative noise are examined. Section 6.2 deals with excitable nets with diffusive coupling in the presence of additive variability.

6.1 Oscillatory Nets of Hodgkin-Huxley Elements

In this section the mean values from Eqs. (3.15) are chosen to be

$$(\Im, \Pi) = (10\mu A, 0.125).$$

Without variability each HH element has the same parameter values $p_{ij} = \Pi$ and $I_{ij} = \Im$ and according to the stability analysis both, the HH elements and the reduced HH elements, are in the oscillatory regime O (Fig. 2.2). Without noise they perform autonomous limit cycle oscillations. In this case the net yields, due to the coupling, a synchronised output (global oscillation) after a transient for nearly all initial conditions.

6.1.1 Additive Variability and Additive Noise

At first the interplay of additive variability and additive noise is studied in a net of HH elements [Eqs. (3.12)] with diffusive coupling [Eq. (2.18)]. The coupling strength is chosen to be $q = 2$, where this small value is sufficient to observe pattern formation, and the side length of the net is $N = 128$. The multiplicative stochastic terms are neglected.

The dynamics of the single HH element strongly depends on its parameter value I_{ij}. For $I_{ij} > 9.8\mu A$ the element is in the oscillatory regime O and for $I_{ij} < 6.3\mu A$ in the excitable regime E. In an area of the parameter space between the excitable and the oscillatory regime one finds the regime $O3$, where a stable focus and a stable limit cycle coexist [white band in Fig. 6.1(a)]. The discussion in this paragraph shows that the oscillatory net of HH elements with additive variability is a mixture of oscillatory and excitable elements.

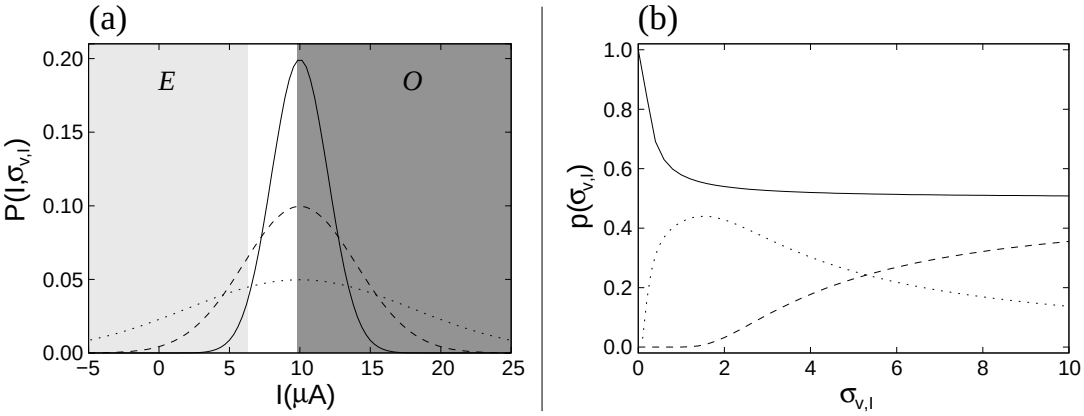

Figure 6.1. (a): The Gaussian probability distribution $P(I, \sigma_{v,I})$ for three different values of the variability strength, (—) $\sigma_{v,I} = 2\mu A$, (- -) $\sigma_{v,I} = 4\mu A$ and (· ·) $\sigma_{v,I} = 8\mu A$. The grey areas mark the dynamical regimes of Eqs. (2.4). (b): Probability $p(\sigma_{v,I})$ for one Hodgkin-Huxley element [Eqs. (2.4)] to be in the oscillatory regime O (—), the excitable regime E (- -) and the regime $O3$ (· ·) in dependency on the variability strength $\sigma_{v,I}$.

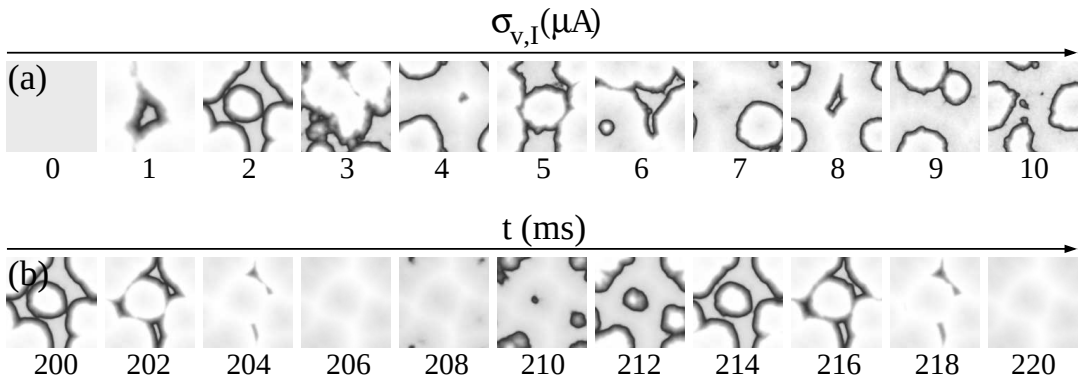

Figure 6.2. Snapshots of $V_{ij}(t)$ for a net of HH elements [Eqs. (3.12)] with diffusive coupling [Eq. (2.18)] for $q = 2$, $N = 128$ and $\sigma_{n,I} = 0\mu A$. Linear grey scale between $V \leq -75.0mV$ (white) and $V \geq 60.0mV$ (black). (a): In dependency on the variability strength $\sigma_{v,I}$ for $t =$

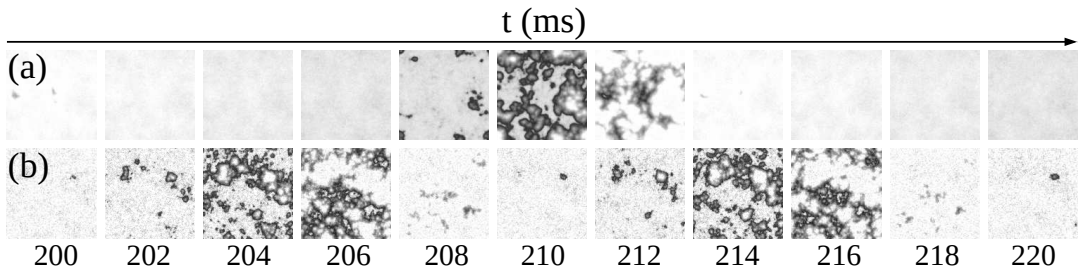

Figure 6.3. Snapshots of $V_{ij}(t)$ for a net of HH elements [Eqs. (3.12)] with diffusive coupling [Eq. (2.18)] in dependency on the integration time t for $q = 2$, $N = 128$ and $\sigma_{v,I} = 2\mu A$. Linear grey scale as in Fig. 6.2. (a): $\sigma_{n,I} = 7\mu A$. (b): $\sigma_{n,I} = 40\mu A$.

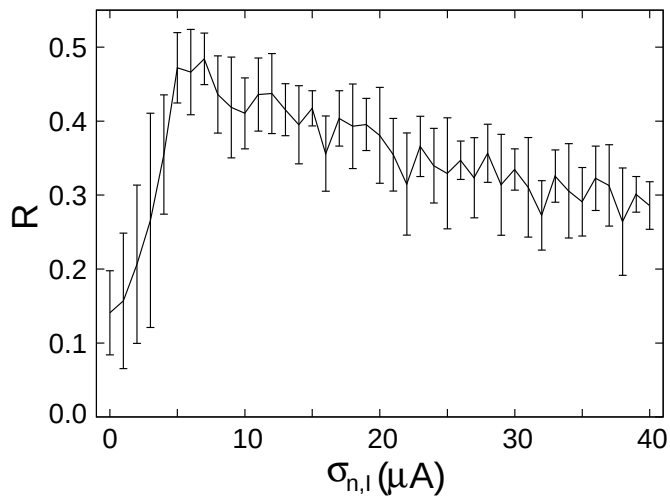

Figure 6.4. The order parameter R [Eq. (2.21)] for a net of HH elements [Eqs. (3.12)] with diffusive coupling [Eq. (2.18)] in dependency on the noise strength $\sigma_{n,I}$, averaged over ten realisations of the net for $q = 2$, $N = 128$ and $\sigma_{v,I} = 2\mu A$.

The probability $p(\sigma_{v,I})$ for an element to be in one of the important dynamical regimes depends on the variability strength $\sigma_{v,I}$ [Fig. 6.1(b)].

In a first step a net without additive noise is studied. Increasing the variability strength for such a net even small values of $\sigma_{v,I}$ induce a coherent pattern formation and the global oscillation is destroyed Fig. 6.2(a). The pattern formation is displayed in Fig. 6.2(b) in detail for $\sigma_{v,I} = 2\mu A$. A further increase of the variability strength has no big influence on the net dynamics and thus on the pattern formation [Fig. 6.2(a)]. The variability induced pattern formation, which is found for a wide range of the coupling strength, is similar to the pattern formation in nets of FHN elements, which was presented in Section 4.1.

With additive noise the dynamics of the heterogeneous net changes completely. This is demonstrated in Fig. 6.3 for the variability strength $\sigma_{v,I} = 2\mu A$ and two values of the noise strength $\sigma_{n,I}$. For the intermediate noise strength $\sigma_{n,I} = 7\mu A$ the variability induced pattern formation, which is presented in Fig. 6.2(b), is destroyed. Instead the net shows a quite regular global oscillation [Fig. 6.3(a)]. A further increase of the noise strength disturbs the regular oscillations and the noise more and more dominates the net dynamics [Fig. 6.3(b)].

To quantify the noise-induced synchronisation in the heterogeneous oscillatory net the order parameter R [Eq. (2.21)], plotted in Fig. 6.4 in dependency on the noise strength for $\sigma_{v,I} = 2\mu A$, is used. The value of R is minimal for $\sigma_{n,I} = 0\mu A$. The additive variability induces pattern formation and therefore the net does not oscillate synchronously. Increasing now the noise strength for such a heterogenous net one finds a sudden increase of the value of R. The noise destroys the pattern formation and leads to a more synchronised oscillation of the net. For $\sigma_{n,I} \approx 6\mu A$ the order parameter R is maximal and the net exhibits thus an optimal synchronisation. A further increase of the noise strength leads to a slow decrease of R. The global oscillation is now more and more disturbed by the noise. The noise-induced synchronisation shows a certain resonance-like behaviour with a maximally synchronised net dynamics at intermediate values of the noise strength.

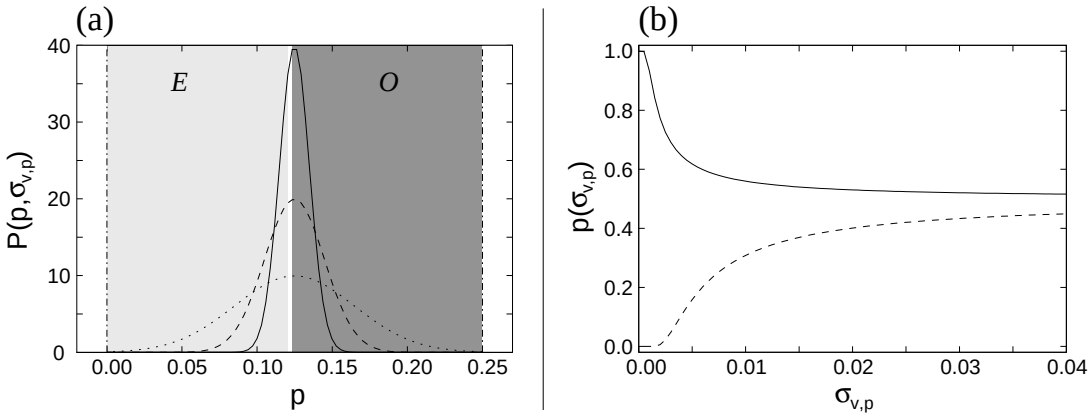

Figure 6.5. (a): The Gaussian probability distribution $P(p, \sigma_{v,p})$ for three different values of the variability strength, (—) $\sigma_{v,p} = 0.01$, (- -) $\sigma_{v,p} = 0.02$ and (· ·) $\sigma_{v,p} = 0.04$. The grey areas mark the dynamical regimes of Eqs. (2.4). (· - ·) cut-off of the probability distribution. (b): Probability $p(\sigma_{v,p})$ for one Hodgkin-Huxley element [Eqs. (2.4)] to be in the oscillatory regime O (—) and the excitable regime E (- -) in dependency on the variability strength $\sigma_{v,p}$.

6.1.2 Multiplicative Variability and Multiplicative Noise

Throughout this subsection the multiplicative stochastic terms are examined, whereas the additive stochastic terms are neglected ($\sigma_{v,I} = 0\mu A$ and $\sigma_{n,I} = 0\mu A$). The oscillatory net with multiplicative variability is a mixture of excitable and oscillatory elements, displayed in Fig. 6.5 for the full HH model [Eqs. (2.4)]. For parameter values smaller than $p \approx 0.12$ the element is excitable for both the HH and the reduced HH model. The border of the oscillatory regime is found for $p \approx 0.1245$ for the HH model and for $p \approx 0.123$ for the reduced model (stability analysis in Fig. 2.2). Between the excitable and the oscillatory regime a small area in parameter space exist, where the regime $O3$ is found. Furthermore, for parameter values $p < 0$, the reaction rate $\beta_n(V)$ [Eqs. (2.4)] is negative and the dynamics of the element completely changes. This is not allowed and consequently the parameter values $p_{ij} < 0$ have to be excluded by setting the probability distribution $P(p, \sigma_{v,p})$ to zero for corresponding values of p. To preserve the symmetry of the probability distribution values of the parameter p greater then 2Π are also excluded [cut-off in Fig. 6.5(a)]. For $\sigma_{v,p} = 0.04$, the largest value of the strength of the multiplicative variability studied in this chapter, this cut-off has nearly no influence on the probability distribution [Fig. 6.5(a)]. The probability to be in one of the two important dynamical regimes depends on the variability strength $\sigma_{v,p}$, displayed in Fig. 6.5(b) for the full model.

For the reduced HH model [Eqs. (2.8)] the probability to be in one of the two important regimes is similar to the coresponding probabilities for the full model. The only difference is that for small values of $\sigma_{v,p}$ the probability to be in the regime O is slightly larger (the border to the regime O is found for a larger value of p).

The systematic influence of the multiplicative noise on the system dynamics can be calculated using the small noise expansion of the HH model [Eq. (3.17)]. The result of a linear stability analysis of this approximation is presented in Fig. 6.6 in dependency on the parameters I and $\sigma_{n,p}$ for both, the HH and the reduced HH model. Increasing the noise strength for $I = 10\mu A$ a transition from the oscillatory regime O to the regime $O3$ takes place. For a further increase of $\sigma_{n,p}$ the dynamics of the system changes again and

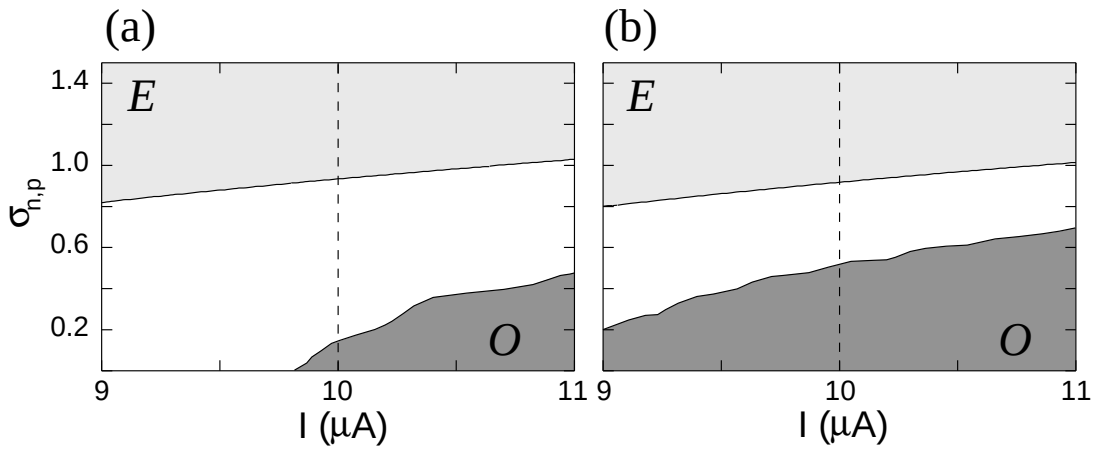

Figure 6.6. Stability analysis of the small noise expansion of the Hodgkin-Huxley model [Eq. (3.17)] in dependency on the parameter I and the noise strength $\sigma_{n,p}$. (a): For the full model [Eqs. (3.12)]. (b): For the reduced model [Eqs. (3.14)]. (—) boundaries of the dynamical regimes, (- -) $I = 10\mu A$. E has one stable focus (excitable regime). O has one unstable focus and one stable limit cycle (oscillatory regime). The white region between E and O is the regime $O3$.

the excitable regime E is realised. The transition from O to $O3$ takes place for $\sigma_{n,p} \approx 0.15$ for the HH model and for $\sigma_{n,p} \approx 0.52$ for the reduced HH model. The difference between the two models is much smaller for the transition from $O3$ to the excitable regime, which is found at $\sigma_{n,p} \approx 0.93$ and $\sigma_{n,p} \approx 0.92$, respectively.

To verify the predictions from the small noise expansion numerical simulations of oscillatory nets of globally coupled [Eq. (2.16)] HH elements for different side lengths N and different coupling strengths q are performed, where all simulations are started with random initial conditions. To identify the transition from oscillatory dynamics to a noise and/or variability induced stable fixed point the time averaged mean field M [Eq. (2.19)] of the Variable $n(t)$ of the HH model is used as an oder parameter. The transition is associated with a jump of the mean field from $M > 0.49$ to $M < 0.4$. This jump is marked by a contour-line for $M = 0.4$, which is denoted with M_c.

Results of the mean field for nets with $N = 50$ varying the coupling strength q and the noise strength $\sigma_{n,p}$ are plotted in Fig. 6.7(a) and (b). One finds $M < M_c$ and thus a stable fixed point for large coupling strengths $q \gtrsim 10$ and sufficiently large noise strengths. The strong coupling is necessary to minimise the random influences of the noise and to stabilise the net in the fixed point. The results for the multiplicative noise in the HH model changing the coupling strength are similar to the results for oscillatory nets of FHN elements presented in Fig. 4.11(a). However for large coupling strengths the noise induced fixed point is found in the middle of the regime $O3$. This is different for the FHN system, where the fixed point was found at the border of the regimes $O3$ and E for simulations with random initial conditions. In the regime $O3$ a stable limit cycle and a stable focus coexist, where the initial conditions and the area of attraction of the two attractors determine whether the limit cycle or the fixed point is found in the simulations. Therefor the numerical results are in agreement with the predictions of the small noise expansion. Furthermore, also in agreement with the theory, the noise induced transition is found for larger values of the noise strength for the reduced model than for the full model.

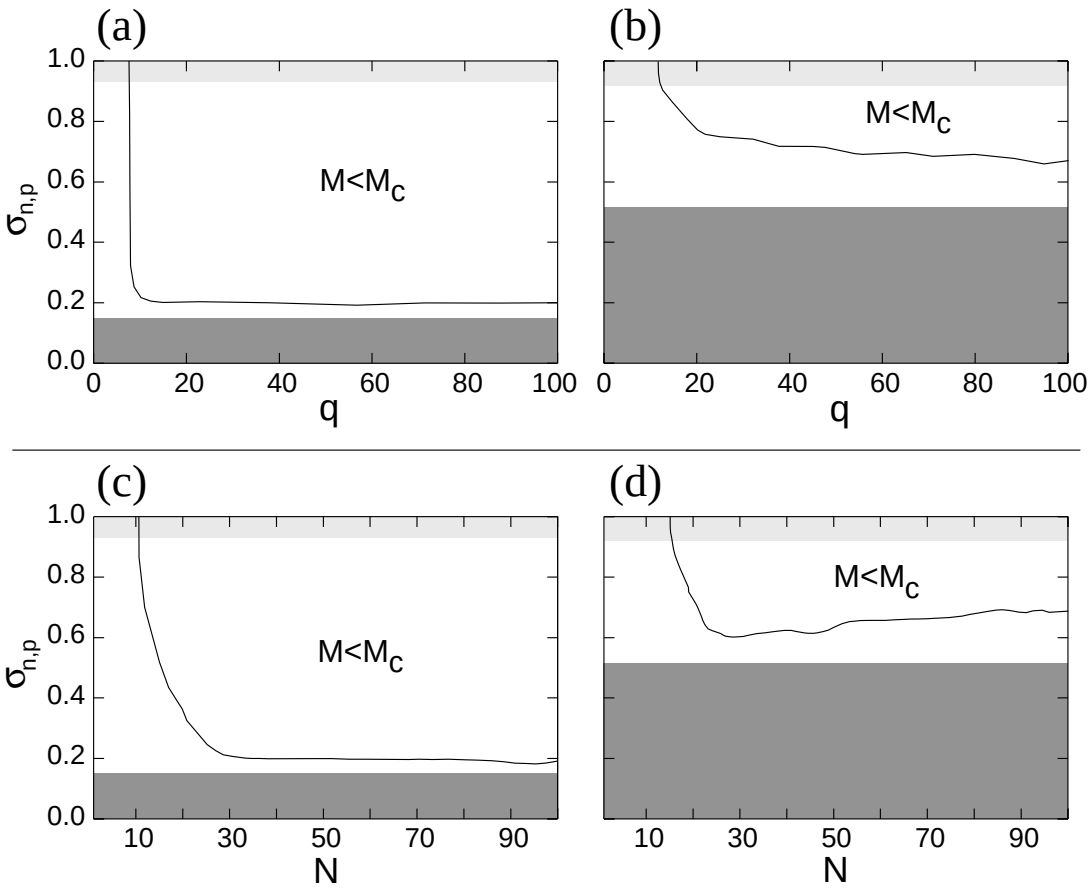

Figure 6.7. The time averaged mean field [Eq. (2.19)] for nets of HH elements with global coupling [Eq. (2.16)] averaged over ten realisations of the net, (—) M_c. The grey areas are the predictions from Eq. (3.17), (light grey) is the regime E, (dark grey) is the regime O, (white) the regime $O3$. (a), (b): In dependency on the noise strength $\sigma_{n,p}$ and the coupling strength q for $N = 50$. (c), (d): In dependency on the noise strength $\sigma_{n,p}$ and the side length N for $q = 50$. (a), (c): For the full model [Eqs. (3.12)]. (b), (d): For the reduced model [Eqs. (3.14)].

Varying the net size for $q = 50$ one finds $M < M_c$ for large enough values of the noise strength and for side length larger than $N \approx 10$ [Fig. 6.7(c) and (d)]. Thus a minimal net size is necessary to find the noise induced stable fixed point. The dynamics of a small net is not determined by the systematic effect, but by the remaining random influences of the noise and hence the regimes $O3$ and E are not found [10, 11]. For a sufficiently large N the transition occurs in the predicted range of the noise strength and the contour line M_c is again, as expected, found for much larger values of $\sigma_{n,p}$ for the reduced model than for the full model.

Studying now the influence of the multiplicative variability for $\sigma_{n,p} = 0$ no simple theoretical prediction exist (see Section 3.3). However according to the results for oscillatory nets of FHN elements, presented in Section 4.2, one expects that the multiplicative variability leads to similar results than the multiplicative noise. This means that one expects to find a variability induced stable fixed point for nets with a sufficiently large coupling strength and net size.

Numerical results for nets with global coupling for $N = 50$ changing the coupling

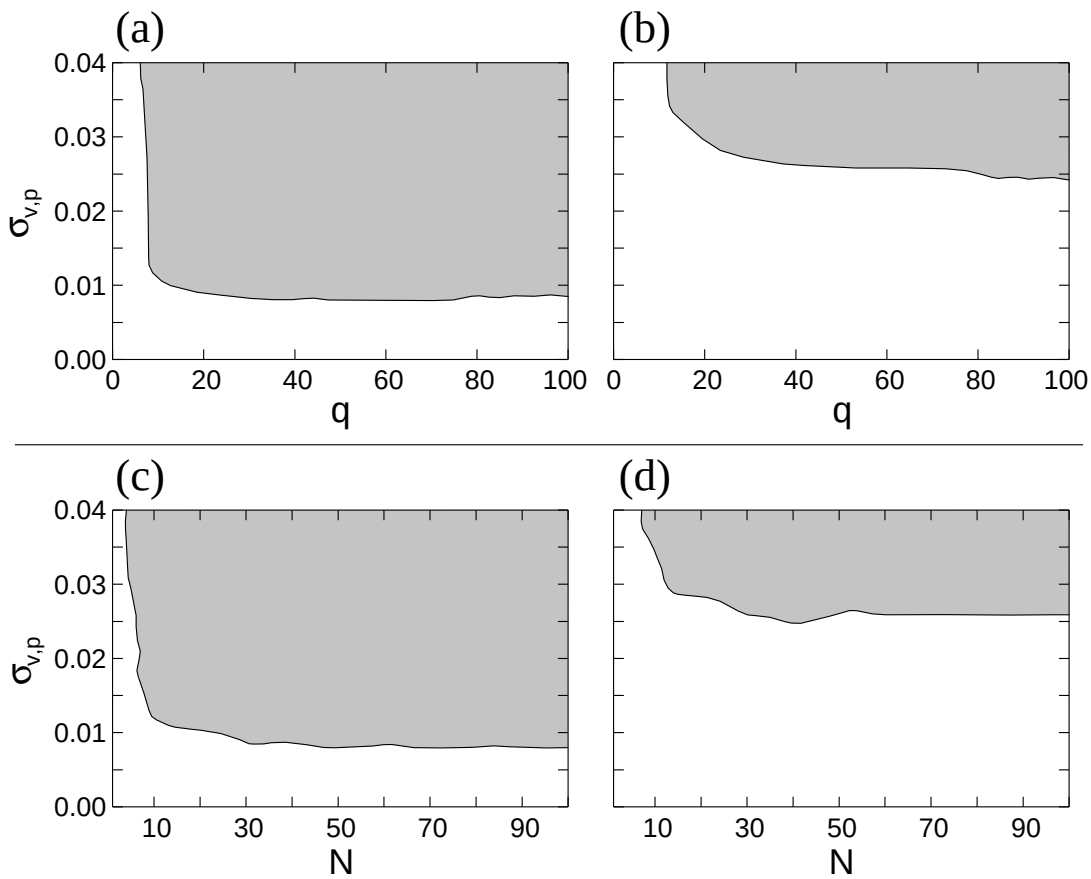

Figure 6.8. The time averaged mean field [Eq. (2.19)] for nets of HH elements with global coupling [Eq. (2.16)] averaged over ten realisations of the net, (—) M_c. The grey area marks $M < M_c$. (a), (b): In dependency on the variability strength $\sigma_{v,p}$ and the coupling strength q for $N = 50$. (c), (d): In dependency on the variability strength $\sigma_{v,p}$ and the side length N for $q = 50$. (a), (c): For the full model [Eqs. (3.12)]. (b), (d): For the reduced model [Eqs. (3.14)].

strength q and the variability strength $\sigma_{v,p}$ are displayed in Fig. 6.8(a) and (b). As expected one finds $M < M_c$ and thus a variability induced stable fixed point for values of the coupling strength larger than $q \approx 10$ for large enough values of the variability strength. Changing now the side length N of the net for a fixed coupling strength $q = 50$ one finds the expected transition for sufficiently large nets with $N \gtrsim 10$ [Fig. 6.8(c) and (d)]. For the reduced model the transition occurs for much larger values of $\sigma_{v,p}$ than for the full model. These findings are in good agreement with the results presented in Fig. 6.7 and Section in 4.2.

Examining now the combined influence of the multiplicative variability and the multiplicative noise on a globally coupled oscillatory net of HH elements with $q = 50$ and $N = 50$ one gets the results of the time averaged mean field presented in Fig. 6.9. The contour line M_c, now a function of $\sigma_{v,p}$ and $\sigma_{n,p}$, reveals an elliptical symmetry. For large values of the variability strength and/or the noise strength a stable fixed point exists. A similar result was found in Section 4.2 (Fig. 4.13) for nets of FHN elements. As expected from the previous results the border to the stable fixed point is found for much larger values of $\sigma_{v,p}$ and/or $\sigma_{n,p}$ for the reduced model than for the full model.

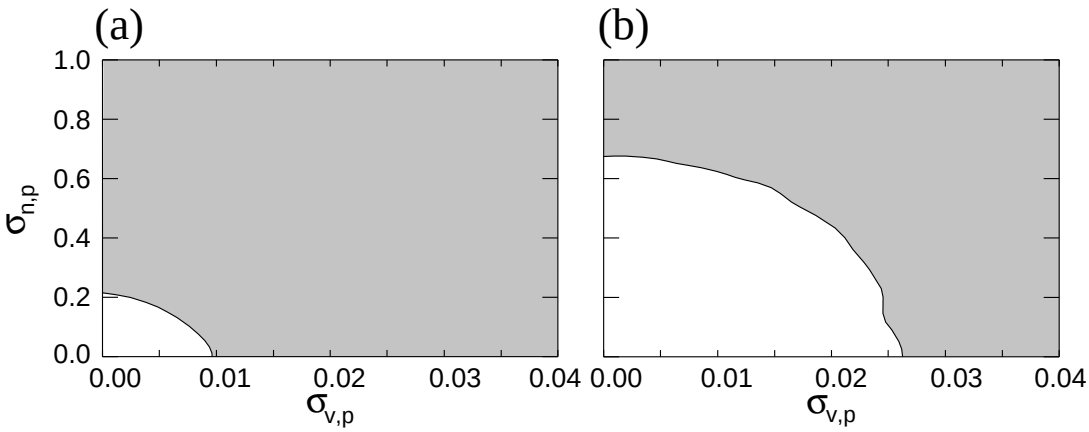

Figure 6.9. The time averaged mean field [Eq. (2.19)] for a net of HH elements with global coupling [Eq. (2.16)] in dependency on the noise strength $\sigma_{n,p}$ and the variability strength $\sigma_{v,p}$ averaged over ten realisations of the net for $q = 50$ and $N = 50$, (—) M_c. The grey area marks $M < M_c$. (a): For the full model [Eqs. (3.12)]. (b): For the reduced model [Eqs. (3.14)].

The results for the globally coupled nets demonstrate that increasing the strength of the multiplicative stochastic terms in large nets with a strong coupling a variability and/or noise induced transition to a regime with a stable fixed point is found. A systematic influence of the stochastic terms on the net dynamics, which can be approximated for the noise via a small noise expansion [Eq. (3.17)], is the reason for this transition.

To examine, whether the variability and/or noise induced transition leads to excitable net dynamics, the influence of the multiplicative stochastic terms on a large diffusively coupled [Eq. (2.18)] oscillatory net with the side length $N = 512$ is studied. Based on the results for globally coupled nets the pattern formation in the net is investigated using the large coupling strength $q = 30$ for the numerical simulations. Small coupling strengths, as in the Sections 6.1.1 and 6.2, are not sufficient to observe the variability and/or noise induced transition to the excitable regime.

The pattern formation found in a net of reduced HH elements [Eq. (3.14)] increasing the variability strength for $\sigma_{n,p} = 0$ is pictured in Fig. 6.10. Without variability and noise the net oscillates synchronously [Fig. 6.10(a)]. Increasing the variability strength the dynamics of the diffusively coupled net changes completely. For intermediate values of the strength of the multiplicative variability the synchronised oscillation is destroyed and pattern formation can be observed. These patterns, which are displayed in Fig. 6.10(b) for $\sigma_{n,p} = 0$ and $\sigma_{v,p} = 0.025$, are circular waves, which travel through the whole net (regime E_P). For even larger values of $\sigma_{v,p}$ the net rests in the variability induced stable fixed point for all times [Fig. 6.10(c)]. However excitation waves can be induced by special initial conditions, shown in Fig. 6.10(d) for a circular wave. The net is hence in the excitable regime E_H.

The pattern formation in Fig. 6.10 is shown for a net of reduced HH elements [Eq. (3.14)] with multiplicative variability only. However one finds similar pattern forming regimes for nets with multiplicative noise. It is not important, if the transitions to the regimes E_P and E_H are induced by the multiplicative variability or the multiplicative noise. For the combined influence of the multiplicative stochastic terms one finds an elliptical symmetry for the pattern forming regimes, as expected from Fig. 6.9. This result

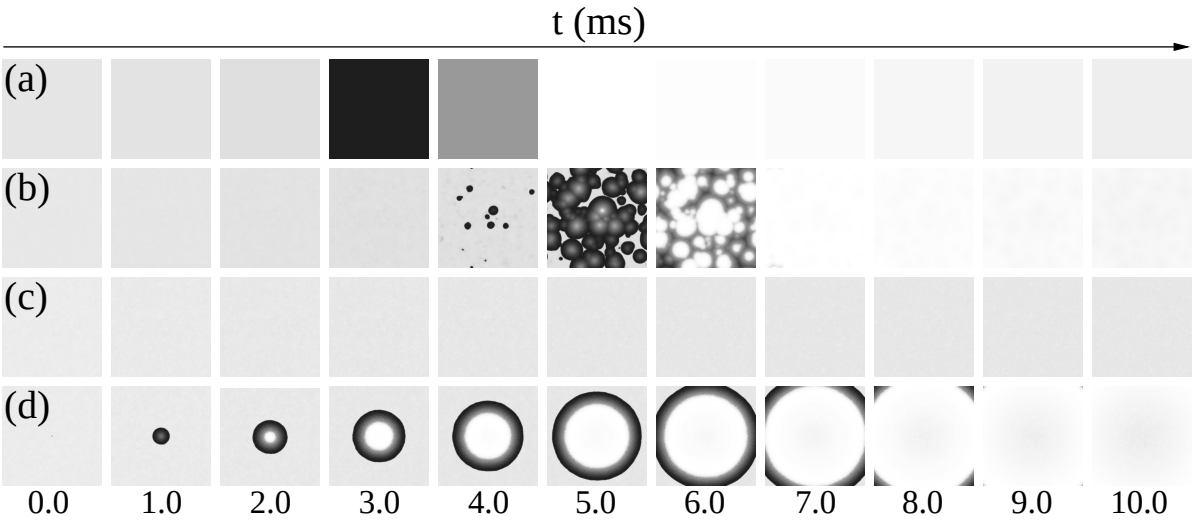

Figure 6.10. Snapshots of $V_{ij}(t)$ for a net of reduced HH elements [Eq. (3.14)] with diffusive coupling [Eq. (2.18)] in dependency on the integration time t for $q = 30$, $N = 512$ and $\sigma_{n,p} = 0$. Linear grey scale between $V \leq -75.0mV$ (white) and $V \geq 60.0mV$ (black). (a): $\sigma_{v,p} = 0$. (b): $\sigma_{v,p} = 0.025$. (c): $\sigma_{v,p} = 0.04$. (d): $\sigma_{v,p} = 0.04$, special initial conditions induce a circular wave.

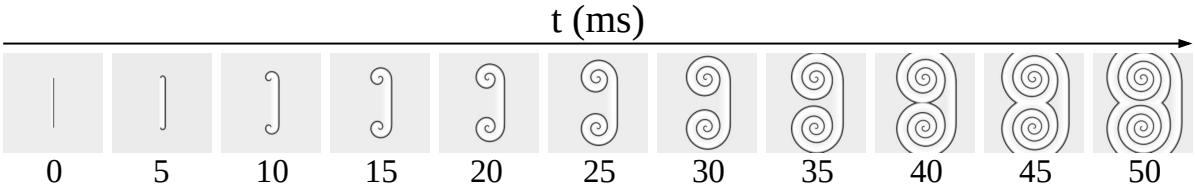

Figure 6.11. Snapshots of $V_{ij}(t)$ for a net of HH elements [Eq. (3.12)] with diffusive coupling [Eq. (2.18)] in dependency on the integration time t for special initial conditions, which induce a spiral wave, for $q = 1$, $N = 256$ and $\sigma_{v,I} = 0\mu A$. Linear grey scale as in Fig. 6.10.

is similar to results found for nets of FHN elements [Fig. 4.15]. The variability and/or noise induced transitions to the regimes E_P and E_H are also found for the full model equations [Eq. (3.12)]. The patterns in the corresponding regimes look thereby similar to the patterns found for the reduced model. For both models the observed transition to excitable dynamics is found in the expected range of the strengths of the stochastic terms. In difference to the FHN model the subexcitable regime E_S is not found for nets of HH elements.

6.2 Excitable Nets of Hodgkin-Huxley Elements

In this section an excitable net of HH elements [Eq. (3.12)] with diffusive coupling [Eq. (2.18)] in the presence of additive variability is studied. The additive noise, the multiplicative noise and the multiplicative variability are neglected and the mean values from Eqs. (3.15) are chosen to be

$$(\Im, \Pi) = (0\mu A, 0.125).$$

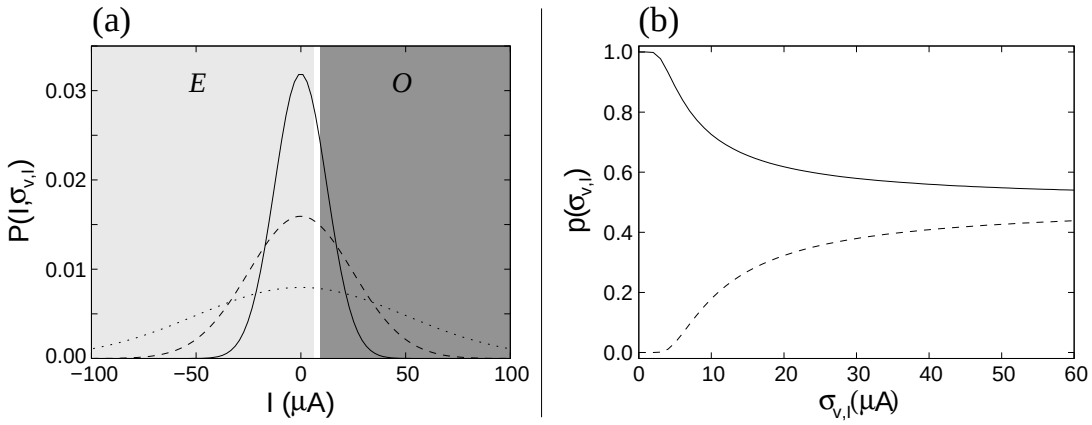

Figure 6.12. (a): The Gaussian probability distribution $P(I, \sigma_{v,I})$ for three different values of the variability strength, (—) $\sigma_{v,I} = 15\mu A$, (- -) $\sigma_{v,I} = 30\mu A$ and (· ·) $\sigma_{v,I} = 60\mu A$. The grey areas mark the dynamical regimes of Eqs. (2.4). (b): Probability $p(\sigma_{v,I})$ for one Hodgkin-Huxley element [Eqs. (2.4)] to be in the excitable regime E (—) and the oscillatory regime O (- -) in dependency on the variability strength $\sigma_{v,I}$.

For $\sigma_{v,I} = 0\mu A$ each HH element is, according to the stability analysis presented in Fig. 2.2(a), in the excitable regime. In the following the coupling strength $q = 1$ and the side length $N = 256$ are used. A time series of a corresponding net is plotted in Fig. 6.11 for $\sigma_{v,I} = 0\mu A$. The net is in the excitable regime E_H and the spiral wave, which is induced by special initial conditions, can propagate through the whole net. The small value of the coupling strength is thus sufficient to observe excitation waves. Increasing the value of q does not lead to qualitatively different results.

In Chapter 5 it is shown that additive variability can induce pattern formation in subexcitable and excitable nets of FHN elements. This variability induced pattern formation exhibits a resonance-like dependency on the variability strength. In this section it is now examined if similar effects are found in an excitable net of HH elements.

The net with additive variability is again a mixture of elements in different dynamical regimes (see Section 6.1.1), what is displayed in Fig. 6.12(a). The probability to be in one of the two important regimes depends on the variability strength $\sigma_{v,I}$ [Fig. 6.12(b)].

Snapshots of the net increasing the variability strength $\sigma_{v,I}$ are composed in Fig. 6.13(a). For variability strengths smaller than $\sigma_{v,I} \approx 20\mu A$ no pattern formation is found and the net remains in the regime E_H [Fig. 6.13(b)]. For slightly larger values of the variability strength the spatial homogeneous solution of the net is not stable anymore. Small clusters of elements in the net oscillate and induce circular waves in the excitable net. A time series for $\sigma_{v,I} = 22\mu A$, displayed in Fig. 6.13(c), shows this coherent pattern formation in detail. Compared to the oscillatory net of HH elements in Section 6.1.1 one needs thus much larger values of the variability strength to induce pattern formation in the excitable net. A further increase of the additive variability leads to more and more oscillatory clusters, which induce circular waves in the net. The wave fronts get smaller and the pattern formation is disturbed by the growing variability strength. For $\sigma_{v,I} = 50\mu A$, a value for which a time series is plotted in Fig. 6.13(d), no coherent pattern formation can be observed anymore.

The variability induced pattern formation in the excitable net of HH elements is, similar to the pattern formation in excitable nets of FHN elements presented in Chapter 5, a

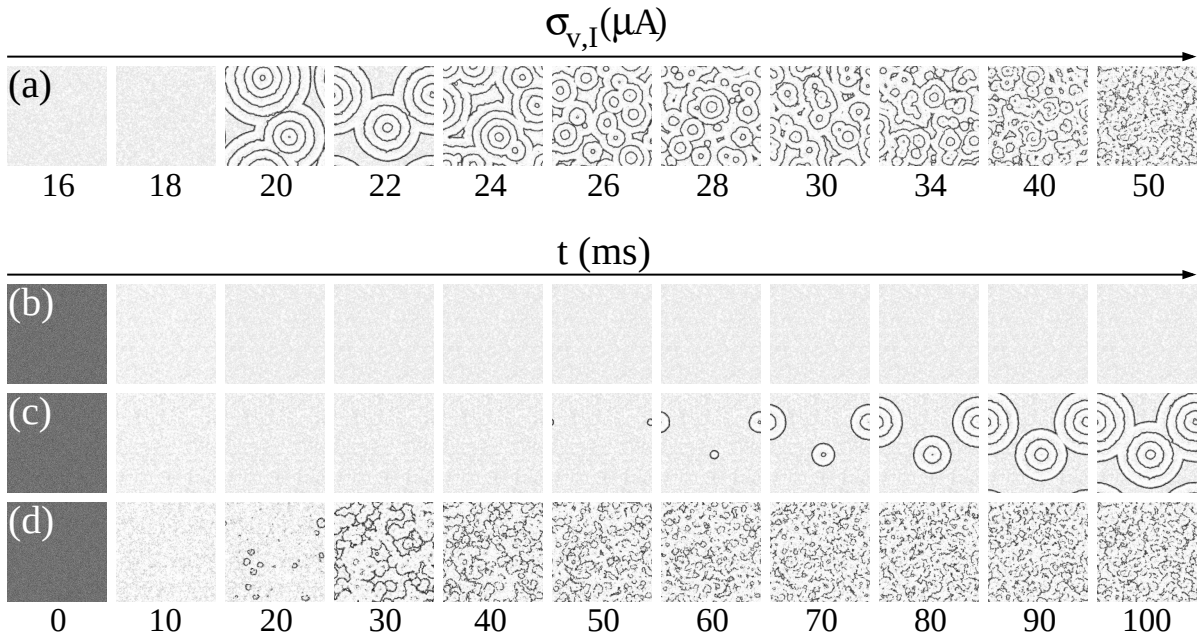

Figure 6.13. Snapshots of $V_{ij}(t)$ for a net of HH elements [Eq. (3.12)] with diffusive coupling [Eq. (2.18)] for random initial conditions, $q = 1$ and $N = 256$. Linear grey scale as in Fig. 6.10. (a): In dependency on the variability strength $\sigma_{v,I}$ for $t = 100ms$. (b)-(d): In dependency on the integration time t for (b) $\sigma_{v,I} = 16\mu A$, (c) $\sigma_{v,I} = 22\mu A$ and (d) $\sigma_{v,I} = 50\mu A$.

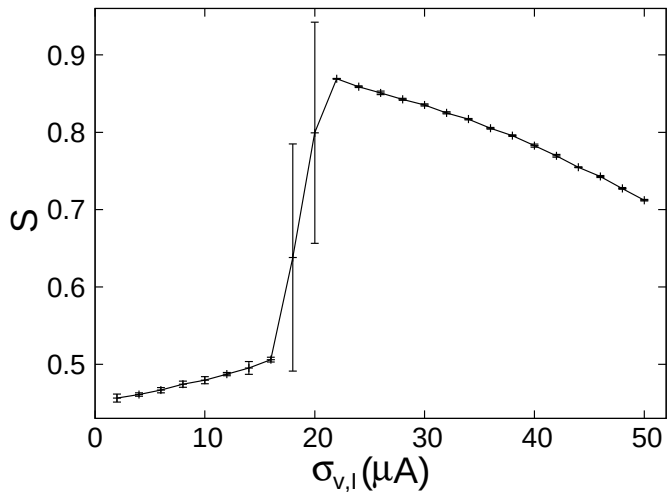

Figure 6.14. The cross correlation S [Eq. (2.24)] for a net of HH elements [Eq. (3.12)] with diffusive coupling [Eq. (2.18)] in dependency on the variability strength $\sigma_{v,I}$, averaged over ten realizations of the net for random initial conditions, $q = 1$ and $N = 256$.

resonance-like effect, where the most coherent patterns are found for intermediate values of the variability strength. Consequently, calculating the cross correlation S [Eq. (2.24)] in dependency on the variability strength $\sigma_{v,I}$, one finds a resonance curve with a maximum at $\sigma_{v,I} \approx 22\mu A$ (Fig. 6.14). The large error bars for $\sigma_{v,I} = 18\mu A$ and $\sigma_{v,I} = 20\mu A$ indicate that for these values of the variability strength the pattern formation is not found for all realisations of the net. For some realisation the spatially homogenous net solutions stays stable.

6.3 Summary and Conclusions

In Section 6.1 it is shown that the interplay of additive variability and additive noise in oscillatory nets of HH elements strongly influences the net dynamics. The additive variability induces pattern formation and hence even small values of the variability strength destroy the synchronised oscillation the net exhibits without variability. In the heterogeneous oscillatory net the synchronisation can be restored by additive noise, where this noise-induced synchronisation exhibits a resonance-like dependency on the noise strength. In the second part of Section 6.1 it was demonstrated that the multiplicative variability and/or the multiplicative noise can induce a transition from oscillatory to excitable dynamics in nets of HH elements. This transition, which has a strong influence on the observed pattern formation, is explained by a systematic influence of the multiplicative stochastic terms. Using a small noise expansion one can predict this systematic influence for the multiplicative noise.

In Section 6.2 it is shown that additive variability can induce coherent pattern formation in excitable nets of Hodgkin-Huxley elements. This pattern formation is a resonance-like effect with maximally coherent patterns for intermediate values of the variability strength.

All the variability and noise induced phenomena presented in this chapter for the more realistic HH model are also found for the FHN model, where the corresponding results are presented and discussed in the Chapters 4 and 5. These phenomena do thus not only appear in one special system, but they are more universal. This finding makes it more likely that similar variability and/or noise induced phenomena may play an important role in oscillatory and excitable biological systems.

As stated in the previous paragraph, the HH model is a more realistic model to describe neuronal dynamics than the FHN model. The model parameters are connected with physical values, which can be measured experimentally. Therefore there is hope that the theoretical findings presented in this chapter provide a starting point to search for the influence of variability and/or noise on pattern formation in real biological systems.

7 Spatially Correlated Variability in Nets of FitzHugh-Nagumo Elements

Coloured noise has been studied in detail in the last years and it was shown that the correlation time and length of a stochastic process may have a strong influence on nonlinear systems. Correlated noise may extend the lifetime of circular waves in subexcitable media [46] or suppress scroll wave turbulences [47]. The correlation of multiplicative noise may strongly influence noise induced transitions [11, 48, 49, 50]. Furthermore, the correlation time and length of additive noise may enhance the pattern formation in subexcitable media [8].

These results motivate to study the influence of coloured variability on spatially extended systems. Thus, in difference to the previous chapters, where only white variability was studied, now the variability is considered to be exponentially correlated [Eqs. (3.4)]. Since one finds for all the results with exponentially correlated variability presented in this chapter similar results for $1/f^{\alpha}$-correlated variability, the results are nearly independent on the special choice of the correlation function.

Throughout this chapter diffusively coupled [Eq. (2.18)] nets of FitzHugh-Nagumo elements [Eqs. (3.1)] with additive and multiplicative variability, but without noise, are studied. The side length of the nets is chosen to be $N = 256$.

The numerical simulations for white variability presented in the previous chapters are done using periodic boundary conditions. The exponentially correlated variability, which is generated using a frequency filtering method, cannot be continued periodically and to avoid a discontinuity at the borders of the net one has to use different boundary conditions. Therefor all simulations with exponentially correlated variability are done using Neumann zero-flux boundaries [8]. This causes excitation waves to vanish at the border of the net.

Studying exponentially correlated variability one has to take care that the maximal correlation length is small compared to the size of the net. Therefor the maximal correlation lengths studied in this thesis are chosen to be $\lambda_{v,e} = 10$ and $\lambda_{v,c} = 10$, what is more than one order of magnitude smaller than the side length of the nets ($N = 256$).

7.1 Additive Variability in Subexcitable Nets

In this section parameter set 2 [Eq. (2.12)] is used. The corresponding stability analysis for a single FitzHugh-Nagumo element in dependency on the parameters e and c is presented in Fig. 2.5(b). The mean values $\mathfrak{E}$ and C of the probability distributions from Eqs. (3.2) are chosen to be

$$(\mathfrak{E}, C) = (-0.3, 4.0). \tag{7.1}$$

Without variability each FHN element has the same parameter values $e_{ij} = \mathfrak{E}$ and $c_{ij} = C$ and the elements are in the regime E. However waves are not sustained in absence of the noise and the net is thus in the subexcitable regime E_S.

Only additive variability is considered ($\sigma_{v,c} = 0$) in this section and the coupling strength is chosen to be $q = 20$. This case was already studied in Section 5.1 for white additive variability, where it is shown that the diverse net, which is a mixture of excitable and oscillatory elements (Fig. 5.1), exhibits pattern formation. Thereby the coherence of the patterns shows a resonance-like dependency on the variability strength $\sigma_{v,e}$ [Fig. 5.4(b)].

The influence of the correlation length $\lambda_{v,e}$ on this variability induced pattern formation is displayed in Fig. 7.1. The lowest row in Fig. 7.1(a) shows again the white variability case ($\lambda_{v,e} = 0$). Increasing now the correlation length the onset of pattern formation is shifted to much smaller values of the variability strength. For white variability the pattern formation sets in for $\sigma_{v,e} \approx 0.12$. For the correlation length $\lambda_{v,e} = 0.5$ one finds the value $\sigma_{v,e} \approx 0.06$, for $\lambda_{v,e} = 1$ the value $\sigma_{v,e} \approx 0.03$ and finally for $\lambda_{v,e} > 5$ the value $\sigma_{v,e} \approx 0.015$. For this small value of the variability strength, as displayed in Fig. 5.1(b), only a few elements in the net are in the oscillatory regime. However, in difference to smaller correlation lengths, the spatially homogeneous solution of the net is unstable. Some elements start to oscillate and act thereby as fixed excitation centres, from which waves spread through the net. After a transient the variability induced patterns in the diverse subexcitable net are periodic in time.

The correlation length does not influence the number of elements in a special regime and thus the number of oscillatory elements depends only on the variability strength $\sigma_{v,e}$ [Fig. 5.1(b)]. The reason, why for a larger correlation length fewer oscillatory elements can induce pattern formation, is visible in Fig. 7.1(b). This figure shows the spatial distribution of the dynamical regimes in the diverse net. For white variability the correlation length is zero and the values of the parameter e, and thus the dynamical regimes of the elements, are randomly distributed in space [lowest row in Fig. 7.1(b)]. A growing correlation length leads to a more and more ordered spatial distribution of the parameter values e_{ij} and thus one finds larger and larger clusters of elements in the oscillatory regime for $\sigma_{v,e} \gtrsim 0.015$. The larger such a cluster is the more likely it starts to oscillate. Therefor for larger values of $\lambda_{v,e}$ the pattern formation occurs for smaller values of the variability strength $\sigma_{v,e}$.

This phenomenon is displayed in more detail in Fig. 7.2 for three different combinations of the correlation length and the variability strength. For white variability ($\lambda_{v,e} = 0$) it is not possible to discern directly from Fig. 7.2(a), where in the net the wave fronts might originate. The oscillatory elements are randomly distributed over the net and they do not form large clusters. Nevertheless for a sufficiently large value of $\sigma_{v,e}$ some elements start to oscillate, probably because of a complicated interplay of the oscillatory elements with elements in the excitable regimes E and $\tilde{E}$. The homogeneous solution of the net is therefor unstable. In the second row, for $\lambda_{v,e} = 1$ and $\sigma_{v,e} = 0.03$, one finds already clusters up to approximately one hundred elements in the regime O, but most of these clusters do still not oscillate. However all the oscillating spots (excitation centres) in Fig. 7.2(b) can be identified as particularly large clusters of oscillatory elements. Most intuitive is the case with $\lambda_{v,e} = 5$, where for the variability strength $\sigma_{v,e} = 0.015$ only one cluster of elements at the lower edge of the net is in the oscillatory regime [lowest picture in Fig. 7.2(a)]. Looking at the corresponding time series in Fig. 7.2(b) one sees that this cluster is oscillating. From this oscillatory centre excitation waves are induced in the subexcitable net.

Increasing the spatial correlation of the variability has a second effect on the pattern formation, which is also visible in the Figs. 7.1 and 7.2. For larger values of $\lambda_{v,e}$ one finds

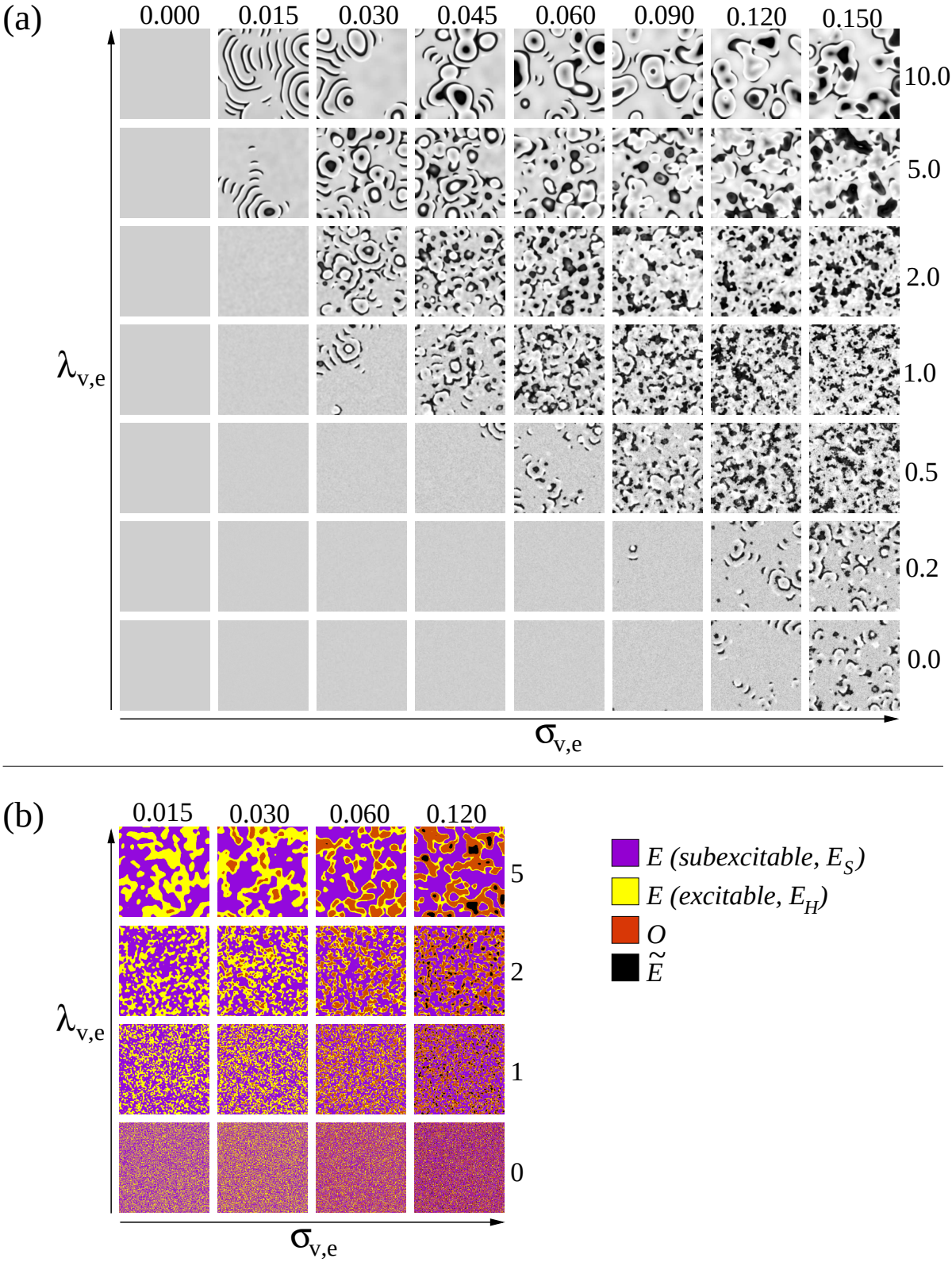

Figure 7.1. Results for a net of FHN elements [Eqs. (3.1)] with diffusive coupling [Eq. (2.18)] in dependency on the variability strength $\sigma_{v,e}$ and the correlation length $\lambda_{v,e}$ for random initial conditions, $t = 50t.u.$, $q = 20$ and $N = 256$. (a): Snapshots of $u_{ij}(t)$. (b): Spatial distribution of the dynamical regimes of the elements in the net coded in a colour-scale.

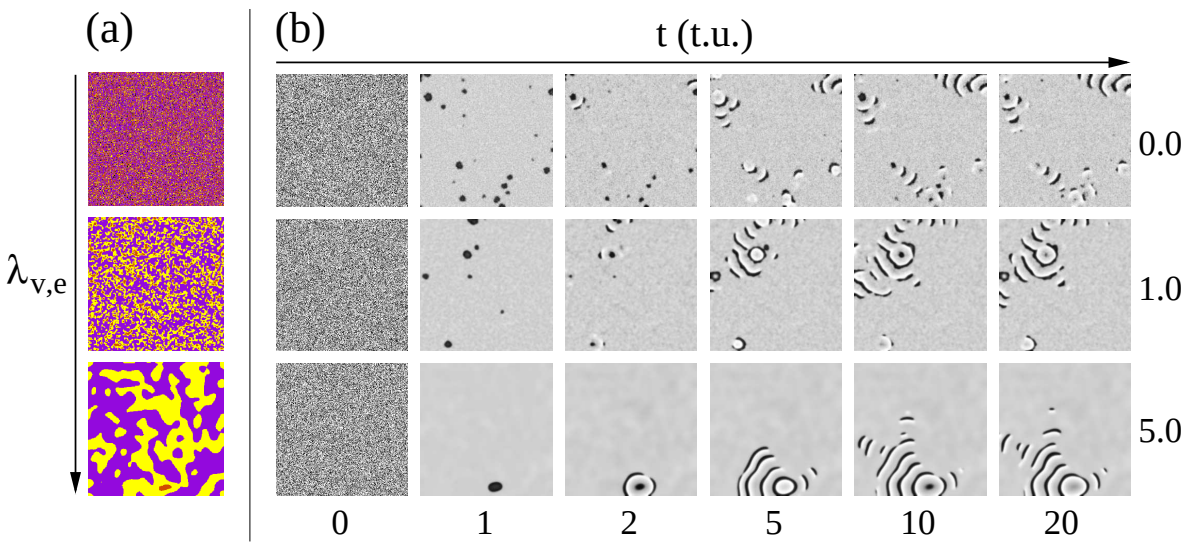

Figure 7.2. Results for a net of FHN elements [Eqs. (3.1)] with diffusive coupling [Eq. (2.18)] in dependency on the integration time t for random initial conditions, $q = 20$ and $N = 256$. (first row) $\sigma_{v,e} = 0.12$ and $\lambda_{v,e} = 0$, (second row) $\sigma_{v,e} = 0.03$ and $\lambda_{v,e} = 1$, (third row) $\sigma_{v,e} = 0.015$ and $\lambda_{v,e} = 5$. (a): Dynamical regimes of the elements in the net coded in a colour-scale [as in Fig. 7.1(b)]. (b): Snapshots of $u_{ij}(t)$.

bigger and more coherent wave fronts, which can travel larger spatial distances through the net. An example of this behaviour is visible in Fig. 7.1 for $\lambda_{v,e} = 10$ and $\sigma_{v,e} = 0.015$, where the excitation waves travel through the whole net. The reason for this phenomenon is that for large correlation lengths large clusters of the net have parameter values e_{ij}, for which these clusters are in the excitable regime E_H [Fig. 7.1(b)]. The oscillatory clusters are always embedded in one of these excitable regions, what is for example visible in Fig. 7.2 for $\lambda_{v,e} = 5$. In this case the single oscillatory cluster induces circular waves in the net, which expand in the excitable region. In some directions the waves can travel much further than in the white variability case, because they do travel mostly through excitable clusters. For some realisations of the net the excitable regions form channels, in which the excitation waves can travel through the the whole net.

For $\sigma_{v,e} < 0.012$ nearly all elements of the net are still in the excitable regime and thus no variability induced pattern formation can be observed. Nevertheless, inducing spiral waves by special initial conditions, the influence of such weak additive variability on wave propagation can be studied. In Fig. 7.3 time series of corresponding wave fronts are plotted for the small variability strength $\sigma_{v,e} = 0.01$ and three correlation lengths $\lambda_{v,e}$.

Without variability the life-time of the induced spiral wave is $t_{lt} = 4.32 t.u.$ and for white variability (first row of Fig. 7.3) one finds that increasing the variability strength leads to a decrease of this life-time. For all correlation lengths $\lambda_{v,e} < 2$ one finds similar results, where one example ($\lambda_{v,e} = 1$) is presented in the second row of Fig. 7.3. For this special realisation of the net the life-time is even shorter than in the white variability case. However for values of the correlation length larger than $\lambda_{v,e} \approx 2$ one observes a completely different influence of the spatial correlation on the life time of the spiral wave. This is displayed in the lowest row of Fig. 7.3 for $\lambda_{v,e} = 5$. In this case the life time of the wave is strongly increased.

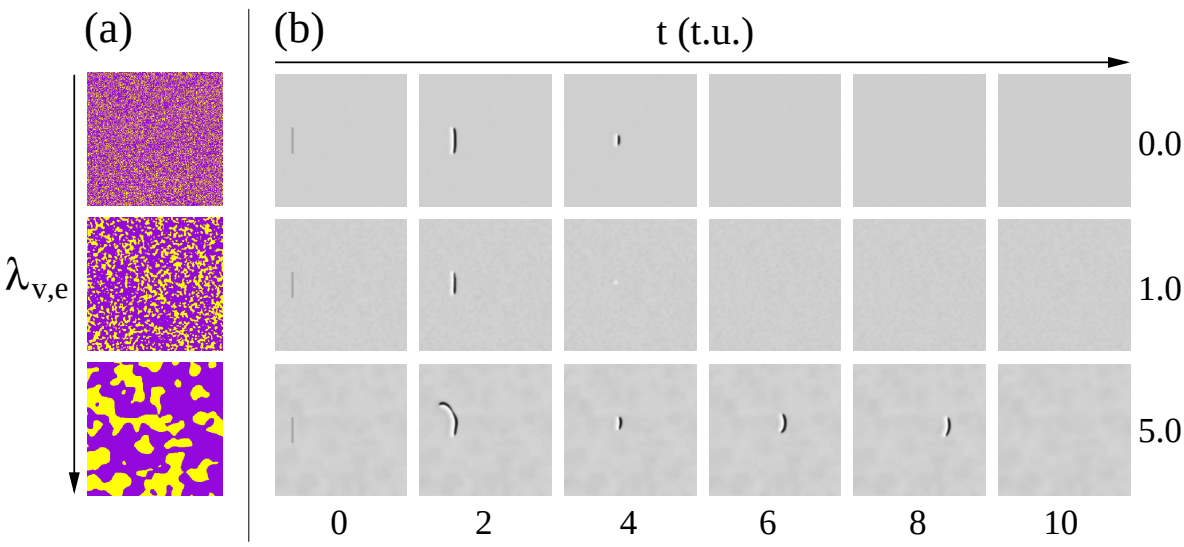

Figure 7.3. Results for a net of FHN elements [Eqs. (3.1)] with diffusive coupling [Eq. (2.18)] in dependency on the integration time t for special initial conditions, which induce a spiral wave, $\sigma_{v,e} = 0.01$, $q = 20$ and $N = 256$. (first row) $\lambda_{v,e} = 0$, (second row) $\lambda_{v,e} = 1$, (third row) $\lambda_{v,e} = 5$. (a): Dynamical regimes of the elements in the net coded in a colour-scale [as in Fig. 7.1(b)]. (b): Snapshots of $u_{ij}(t)$.

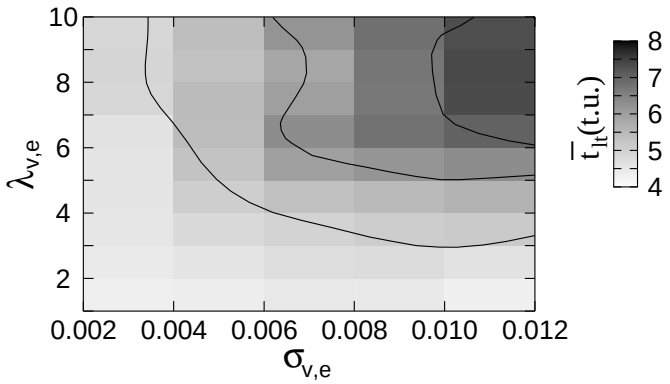

Figure 7.4. Mean life-time $\bar{t}_{lt}$ of spiral waves, which are induced by special initial conditions, for a net of FHN elements [Eqs. (3.1)] with diffusive coupling [Eq. (2.18)] in dependency on the variability strength $\sigma_{v,e}$ and the correlation length $\lambda_{v,e}$ averaged over one hundred realisations of the net for $q = 20$ and $N = 256$.

The reason for the strong increase of the life-time is again that for a growing correlation length larger clusters of the net are excitable [Fig. 7.3(a)] and allow for wave propagation with increasing wave fronts. This phenomenon can be seen in the last row of Fig. 7.3. The wave travels along an excitable region through the net. At the point, where the excitable region ends and an subexcitable part of the net begins, the wave dies out. The special configuration of the net and the place in the net, where the wave is induced, have thus a strong influence on the life-time of the wave. One finds examples of nets with large correlation lengths, where the induced spiral waves dies out after $t_{lf} \approx 1t.u.$, and other examples for identical parameter values, where the waves travels through the whole net.

To get a quantitative measure of the influence of the correlation length $\lambda_{v,e}$ on the net dynamics the mean life-time $\bar{t}_{lt}$ of the spiral waves is calculated (Fig. 7.4). The maximal life-time of a spiral wave is limited by the size of the net. A wave travelling through the whole net can live approximately $10t.u.$ and thus the maximal mean life-time is $\bar{t}_{lt} \approx 10t.u.$. One finds that for $\lambda_{v,e} > 3$ the mean life-time strongly depends on the correlation length and the variability strength. An increase of $\lambda_{v,e}$ and $\sigma_{v,e}$, respectively, leads to an increase of the mean life-time. The largest value of the mean life-time $\bar{t}_{lt} \approx 8t.u.$ is found for maximal values of $\sigma_{v,e}$ and $\lambda_{v,e} > 7$. A further increasing of the correlation length has nearly no influence on the mean life-time. For even larger values of the variability strength the net itself can induce excitation waves (Fig. 7.1).

This result shows that optimal values of the variability strength $\sigma_{v,e}$ and the correlation length $\lambda_{v,e}$ can strongly increase the ability of a subexcitable net to support excitation waves. In the optimal range of these two parameters one gets the double mean life-time $\bar{t}_{lt} \approx 8t.u.$ compared to a corresponding net without variability.

7.2 Multiplicative Variability in Oscillatory Nets

In this section an oscillatory diffusively coupled net of FHN elements with the coupling strength $q = 50$ is studied. Thereby the same parameter values of the FHN model as in Chapter 4 are chosen. This means that parameter set 1 [Eq. (2.11)] is used and that the mean values of the parameters e and c are $(\mathfrak{E}, C) = (0, 4.6)$ [Eqs. (3.2)]. According to the stability analysis [Fig. 2.5(a)] the elements of a net without variability are in the regime O and without noise they perform autonomous limit cycle oscillations. In this case the net yields a synchronised output (global oscillation) after a transient for nearly all initial conditions [Fig. 2.7(a)].

In the previous section it is shown that the correlation length of additive variability might have an essential influence on the dynamics of biophysical networks. Now the correlation length of multiplicative variability is examined, whereas the additive fluctuations ($\sigma_{n,e} = 0$ and $\sigma_{v,e} = 0$) and the multiplicative noise ($\sigma_{n,c} = 0$) are neglected.

Studying exponentially correlated multiplicative variability in parameter c of the FHN model one has to exclude the parameter values $c_{ij} < 0$ and $c_{ij} > 2C$ (Section 4.2). The frequency filtering method used in this thesis to generate the correlated variability does not yield these conditions, therefore one has to set all values $c_{ij} < 0$ to zero and all $c_{ij} > 2C$ to $2C$. For the largest variability strength used in this section, this affects approximately 4% of the Gaussian distributed parameter values.

White multiplicative variability induces a transition from oscillatory to excitable net dynamics (Chapter 4). Thereby one finds pattern formation for intermediate values of the variability strength (Fig. 4.15). Now the influence of the correlation length on the transition to excitability is studied. The results are displayed in Fig. 7.5, where the white variability case ($\lambda_{v,c} = 0$) is plotted in the lowest row. One discerns that even the small correlation length $\lambda_{v,c} = 0.2$ has a distinct influence on the net dynamics. The regime E_H is reached for much larger values of the variability strength compared to the white variability case. The increasing correlation length leads, as displayed in Fig. 7.6, to the formation of larger clusters of elements in the same dynamical regime. For that reason one needs a larger variability strength $\sigma_{v,c}$ for $\lambda_{v,c} = 0.2$ to suppress the dynamics of the clusters in the regimes O and $\tilde{E}$ and to stabilise the temporally constant spatially homogeneous solution. For $\lambda_{v,c} \geq 0.5$ the temporally constant spatially homogeneous

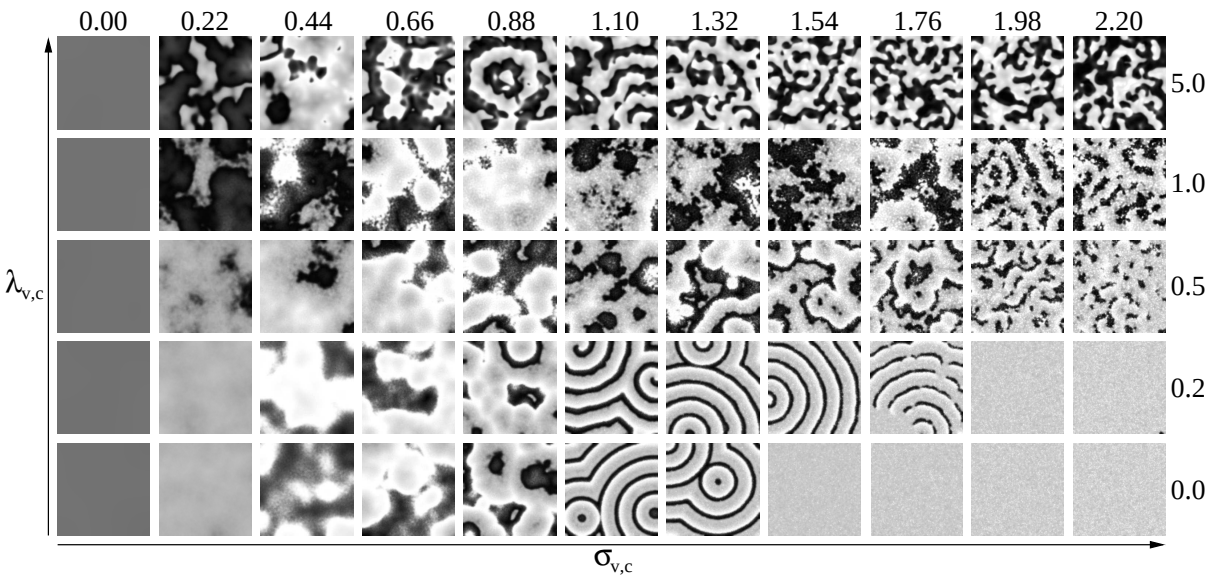

Figure 7.5. Snapshots of $u_{ij}(t)$ for a net of FHN elements [Eqs. (3.1)] with diffusive coupling [Eq. (2.18)] in dependency on the variability strength $\sigma_{v,c}$ and the correlation length $\lambda_{v,c}$ for random initial conditions, the integration time $t = 50t.u.$, $q = 50$ and $N = 256$.

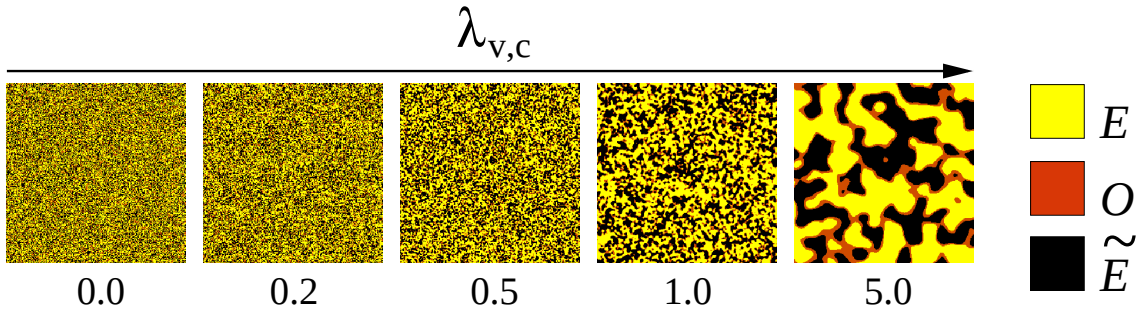

Figure 7.6. Spatial distribution of the dynamical regimes for a net of FHN elements [Eqs. (3.1)] with diffusive coupling [Eq. (2.18)] in dependency on the correlation length $\lambda_{v,c}$ for $\sigma_{v,c} = 1.76$ and $N = 256$. The dynamical regimes are coded in a colour-scale.

solution is unstable for all values of the variability strength and the regimes E_H and E_S do not exist anymore. Furthermore one discerns that the variability induced pattern formation is less coherent than for smaller correlation lengths.

For values of the correlation length $\lambda_{v,c} \geq 1$ one can not identify a transition from oscillatory to excitable net dynamics. In this case increasing the variability strength still leads to pattern formation, where the patterns, which do not look like excitation waves anymore, are a result of the interplay of the large oscillatory and excitable clusters in the net (Fig. 7.6). In such nets the dynamics is not determined by the effective parameter $\langle c \rangle$ and thus one cannot predict the dynamics of the net anymore.

These results demonstrate that an increasing correlation length of the multiplicative variability disturbs the variability induced transition from oscillatory to excitable dynamics in diffusively coupled nets. For $\lambda_{v,c} \geq 0.5$ the regimes E_H and E_S do not exist anymore.

One finds similar results for correlated multiplicative variability in subexcitable nets with parameter values as in Section 5.2, where no clear transition from subexcitable net dynamics to the regime E_H is found for large correlation lengths.

7.3 Summary and Conclusions

In Section 7.1 it is shown that an increasing correlation length of the additive variability can strongly reduce the strength of the additive variability, which is required to induce pattern formation in subexcitable nets. This makes it much more likely that additive variability might play a role for pattern formation in biological systems. Furthermore a large correlation length can strongly increase the mean-life time of excitation waves in subexcitable nets. In this way additive variability may improve the information transfer in such nets. From these results one can conclude that a large spatial correlation can strongly increase the influence of the additive variability on the net dynamics.

Studying the correlation length of multiplicative variability one finds completely different results (Section 7.2). In this case increasing the correlation length disturbs the variability induced transitions from oscillatory to excitable dynamics. This implies that variability induced transitions in diffusively coupled nets can only be observed, if the correlation length of the variability is small compared to the other length scales of the system.

In general one can conclude that the correlation length of the variability may have a crucial influence on the dynamics of diffusively coupled biophysical networks. It might be particularly important for pattern forming mechanism.

8 Variability in the Coupling Strength of Nets of FitzHugh-Nagumo Elements

In the previous chapters it is demonstrated that the kind of coupling, which is considered to be diffusive or global in this thesis, and the coupling strength have a strong influence on the dynamics of nets with variability and/or noise. However these two kinds of coupling are not the only possible choices. In theoretical physics more complicated coupling functions are studied and thereby the topology of a system may be changed [69, 70]. The topology may have a strong influence on the dynamics of spatially extended systems [71, 72]. Furthermore the connectivity and the degree distribution regulate the distribution patterns of excitable systems on graphs [73].

In this chapter variability in the coupling strength is studied in oscillatory nets of FHN elements with nearest-neighbour coupling [Eq. (2.18)]. No natural, in particular biological, system has a perfectly homogeneous regular coupling and thus the coupling strength may vary from element to element in a net. The model equations for a net of FitzHugh-Nagumo elements [Eqs. (3.1)] with variability in the coupling read:

$$\begin{aligned} \dot{u}_{ij} =& \frac{1}{\epsilon}\left[u_{ij}(1-u_{ij})(u_{ij}-a) - v_{ij} + d\right] + q_{ij}K(u_{ij}) \\ \dot{v}_{ij} =& u_{ij} - c_{ij}[1+\eta_{ij}(t)]v_{ij} + e_{ij} + \xi_{ij}(t). \end{aligned} \tag{8.1}$$

Due to the variability the values q_{ij} of the coupling strength q can change from element to element. The parameter values are Gaussian distributed numbers and the parameter Q, with

$$\langle q_{ij} \rangle = Q, \tag{8.2}$$

is the mean value of the Gaussian distribution $P(q, \sigma_{v,q})$. In the following $\sigma_{v,q}$, the standard deviation of the Gaussian distribution, denotes the strength of the variability in the coupling.

In this thesis inhibitoric coupling is not considered and hence negative values of the coupling strength are not allowed. This means that the probability distribution $P(q, \sigma_{v,q})$ has to be set to zero for $q < 0$. To preserve the symmetry of the probability distribution values $q > 2Q$ are also omitted. In Fig. 8.1 corresponding probability distributions are plotted for the two different values of Q, which are studied in this chapter.

Troughout this chapter parameter set 1 [Eq. (2.11)] and the mean values $(\mathfrak{E}, C) = (0, 4.6)$ [Eqs. (3.2)] are used. Nets of FHN elements with these parameter values have been studied already in Chapter 4 and in Section 7.2. According to the stability analysis [Fig. 2.5(a)] the elements of a net without variability are in the regime O and without noise they perform autonomous limit cycle oscillations. In this case the net yields a synchronised output after a transient for nearly all initial conditions [Fig. 2.7(a)]. The influence of the variability in the coupling on the net dynamics is studied using diffusively coupled [Eq. (2.18)] nets of FHN elements with the side length $N = 256$.

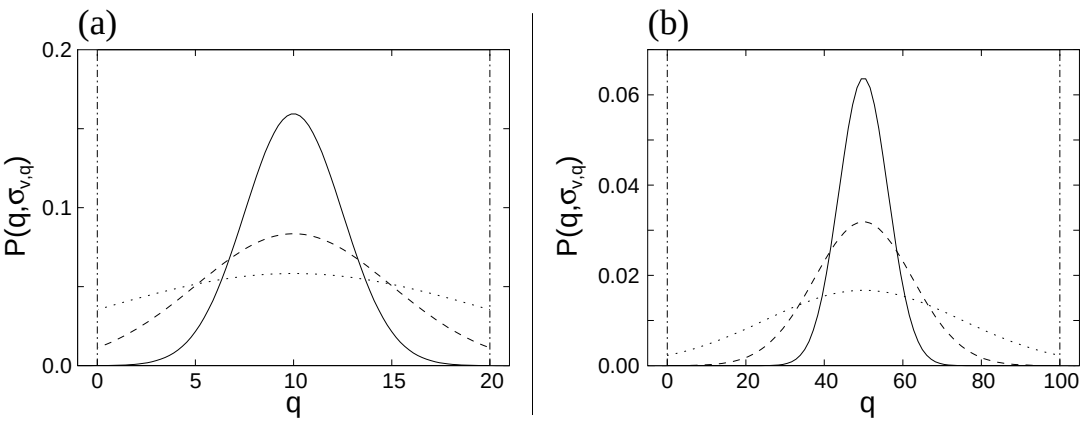

Figure 8.1. The probability distribution $P(q, \sigma_{v,q})$ in dependency on the coupling strength q, $(\cdot\,\text{-}\,\cdot)$ cut-off of the probability distribution. (a): $P(q, \sigma_{v,q})$ for $Q = 10$ and three different values of the variability strength, (—) $\sigma_{v,q} = 2.5$, (- -) $\sigma_{v,q} = 5$ and $(\cdot\ \cdot)$ $\sigma_{v,q} = 10$. (b): $P(q, \sigma_{v,q})$ for $Q = 50$ and three different values of the variability strength, (—) $\sigma_{v,q} = 6.25$, (- -) $\sigma_{v,q} = 12.5$ and $(\cdot\ \cdot)$ $\sigma_{v,q} = 25$.

8.1 Pattern Formation Induced by Variability in the Coupling

In this section the mean of the coupling strength is chosen to be $Q = 10$. The influence of the variability in the coupling is studied in a net with weak additive noise, where the noise strength is set to $\sigma_{n,e} = 0.04$. The additive variability, the multiplicative variability and the multiplicative noise are neglected ($\sigma_{v,e} = 0$, $\sigma_{v,c} = 0$ and $\sigma_{n,c} = 0$).

Without variability in the coupling the net oscillates in a synchronised manner. This global oscillation is slightly disturbed, as shown in Fig. 4.4(a), by the weak additive noise. Therefor looking at snapshots of the net, which are plotted in Fig. 8.2(a), no pattern formation can be observed for $\sigma_{v,q} = 0$. For variability strengths $\sigma_{v,q} < 3$ no significant influence of the variability on the net dynamics can be seen. This changes abruptly for values of the variability strength larger than $\sigma_{v,q} \approx 4$. In this case the net exhibits coherent pattern formation. One can observe circular and more often spiral phase-waves. A time series of such a spiral wave for $\sigma_{v,q} = 5$ is presented in Fig. 8.2(b). The variability induced spiral, which rotates around its centre, is a stable solution of the net. For even larger values of the variability strength $\sigma_{v,q}$ more, but smaller, wave fronts originate. One nevertheless finds coherent pattern formation for all values of the variability strength larger than $\sigma_{v,q} \approx 4$.

In a next step the pattern formation is analysed quantitatively using the synchronisation measure R [Eq. (2.21)] and the cross correlation S [Eq. (2.24)]. Fig. 8.3 shows these quantities in dependency on the variability strength $\sigma_{v,q}$. The order parameter R is maximal for a net without variability, indicating the maximally synchronised oscillations of the noisy net. Up to $\sigma_{v,q} \approx 2$ the value of R is independent of the variability strength and the variability in the coupling has thus no influence on the synchronisation. For $2 < \sigma_{v,q} < 4$ the value of R drops strongly, pattern formation sets in and the synchronisation is destroyed. For values of the variability strength larger than $\sigma_{v,q} \approx 4$ the net exhibits coherent pattern formation and the value of R is minimal, indicating the loss of the global synchronisation. For these large values of the variability strength R is again independent

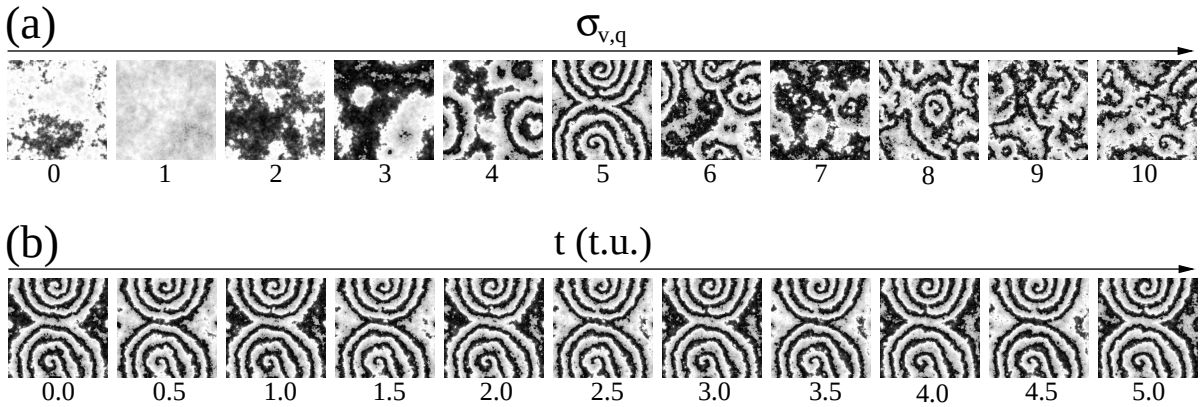

Figure 8.2. Snapshots of $u_{ij}(t)$ for a net of FHN elements [Eqs. (8.1)] with diffusive coupling [Eq. (2.18)] for $\sigma_{n,e} = 0.04$, $Q = 10$ and $N = 256$. (a): In dependency on the variability strength $\sigma_{v,q}$ for the integration time $t = 200t.u.$. (b): In dependency on the integration time t for $\sigma_{v,q} = 5$, the transient is excluded.

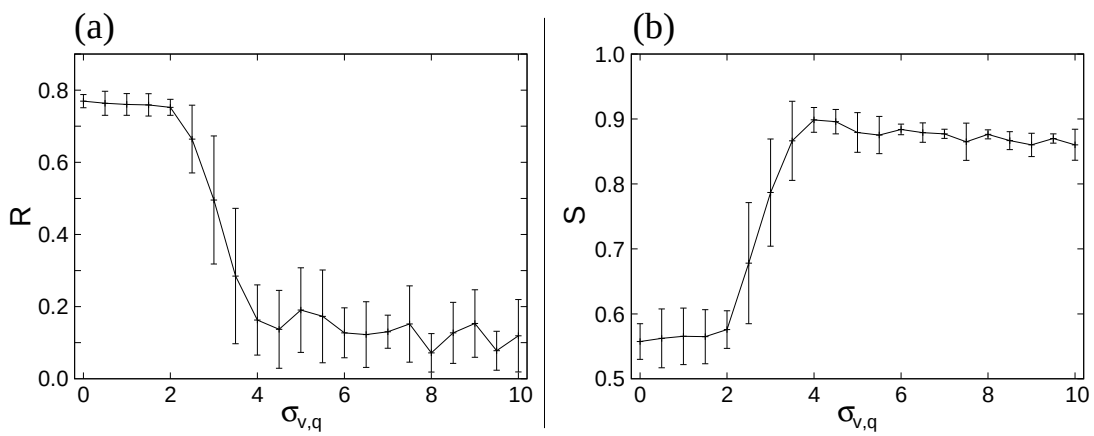

Figure 8.3. Results for a net of FHN elements [Eqs. (8.1)] with diffusive coupling [Eq. (2.18)] in dependency on the variability strength $\sigma_{v,q}$ averaged over ten realisations of the net for $\sigma_{n,e} = 0.04$, $Q = 10$ and $N = 256$. (a): The order parameter R [Eq. (2.21)]. (b): The cross correlation S [Eq. (2.24)].

of $\sigma_{v,q}$.

The cross correlation S, which is plotted in Fig. 8.3(b), shows a reverse dependency on the variability strength than the measure R. One finds the minimal value of S for $\sigma_{v,q} = 0$ and consequently no pattern formation is found in the net. The value of the cross correlation is nearly constant for variability strengths $\sigma_{v,q} < 2$. For $2 < \sigma_{v,q} < 4$ one finds a sudden increase of S, because the variability starts to induce pattern formation. For values $\sigma_{v,q} > 4$, for which the coherent patterns can be observed, the cross correlation is maximal and again nearly independent of the variability strength.

The results presented in this section show that the variability in the coupling strongly influences the dynamics of the oscillatory net. However the variability induced pattern formation emerges only for very large values of $\sigma_{v,q}$. Looking at Fig. 8.1(a) one discerns that the probability distribution $P(q, \sigma_{v,q})$ is already broad for $\sigma_{v,q} = 2.5$, a value of the variability strength, for which one sees nearly no influence of the variability on the net dynamics. For $\sigma_{v,q} = 5$, a value for which coherent pattern formation is found, the probability distribution stretches over the whole allowed range of the coupling strength. Therefore some elements of the net have a small value of the coupling strength ($q_{ij} \lesssim 1$) and are hardly coupled to the rest of the net. These elements can oscillate freely without being influenced by their neighbour elements and thus they do not synchronise with the net. Nevertheless they can still influence the dynamics of their neighbour elements and thus they disturb the synchronised dynamics of the net and lead to the observed coherent pattern formation.

Excluding the small values of the coupling strength using different cut-off values of $P(q, \sigma_{v,q})$ (Fig. 8.1), for example $q = 2$ and $q = 18$ instead of $q = 0$ and $q = 20$, one does not find a variability induced coherent pattern formation. It is thus not the broad distribution of the q_{ij} but the single elements with very small values of the coupling strength, which lead to the observed pattern formation.

8.2 Interplay of Variability in the Coupling and Multiplicative Variability

In this section the mean of the coupling strength of the oscillatory net of FHN elements is chosen to be $Q = 50$ [Fig. 8.1(b)]. In Chapter 4 it was demonstrated that multiplicative variability can induce a transition from oscillatory to excitable net dynamics for the chosen parameter values. Now the interplay of the multiplicative variability with the variability in the coupling is examined. The additive stochastic terms and the multiplicative noise are neglected ($\sigma_{n,e} = 0$, $\sigma_{v,e} = 0$ and $\sigma_{n,c} = 0$).

In Fig. 8.4 snapshots of the net for different values of the variability strengths $\sigma_{v,c}$ and $\sigma_{v,q}$ are plotted. The lowest row ($\sigma_{v,q} = 0$) shows again the variability induced transition from oscillatory to excitable dynamics, which was studied in detail in Section 4.2. The regime E_P is found for intermediate values of $\sigma_{v,c}$. Increasing now the variability in the coupling for a given value of $\sigma_{v,c}$ one sees nearly no influence on the net dynamics for $\sigma_{v,q} < 10$. For values of the variability strength $10 \leq \sigma_{v,q} \leq 15$ the variability in the coupling has still no influence on the net dynamics for $\sigma_{v,c} = 0$ and thus one finds in this case an undisturbed synchronised oscillation. Increasing the strength of the multiplicative variability for these values of $\sigma_{v,q}$ the expected transition to the excitable regime is found. The only difference to the case $\sigma_{v,q} = 0$ is that the regime E_P is realised for a broader range of the variability strength $\sigma_{v,c}$. The coupling of some of the oscillatory elements to

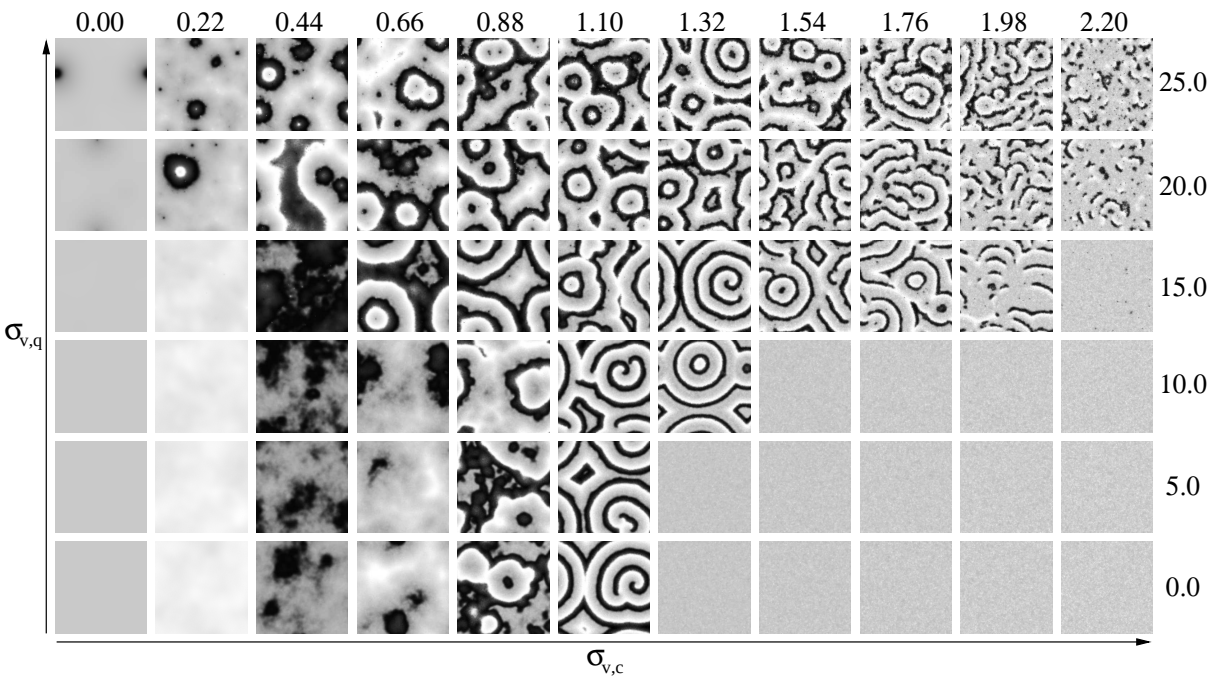

Figure 8.4. Snapshots of $u_{ij}(t)$ for a net of FHN elements [Eqs. (8.1)] with diffusive coupling [Eq. (2.18)] in dependency on the variability strength $\sigma_{v,c}$ and the variability strength $\sigma_{v,q}$ for the integration time $t = 50t.u.$, $Q = 50$ and $N = 256$.

the rest of the net is weaker than for the homogeneous coupling. These elements oscillate and induce excitation waves, in contrast to the case $\sigma_{v,q} = 0$ and $\sigma_{v,c} \geq 1.32$, where the spatially homogeneous temporally constant solution of the net is stable.

For even larger values of $\sigma_{v,q}$ ($\sigma_{v,q} \geq 20$) the variability in the coupling can induce pattern formation in nets with weak multiplicative variability ($\sigma_{v,c} \leq 0.44$). This phenomenon is equivalent to the one presented in Section 8.1 for a different value of Q. The mechanism of the pattern formation is explained there. One furthermore notes that the spatially homogeneous temporal constant solution of the net is now unstable for all values of $\sigma_{v,c}$. For these large values of $\sigma_{v,q}$ some oscillatory elements have a so small value of the coupling strength that they are barely influenced by their neighbour elements [Fig. 8.1(b)]. Theses elements oscillate and induce waves in the excitable net, where the size of the wave fronts is controlled by the multiplicative variability.

8.3 Summary and Conclusions

In Section 8.1 it is shown that variability in the coupling can induce coherent pattern formation in oscillatory nets of FHN elements. These patterns are only found, if the variability is so strong that some elements oscillate freely, because they are barely coupled to their neighbour elements anymore. In the second section of this chapter the interplay of variability in the coupling and multiplicative variability was studied. The variability in the coupling is able to disturb the transition from oscillatory to excitable dynamics, which is caused by the multiplicative variability.

The results presented in this chapter show that variability in the coupling may have an influence on the dynamics of spatially extended systems. However the strength of the

variability has to be very large to see such influences. For small values of $\sigma_{v,q}$ the dynamics of the observed nets are very robust under the influence of variability in the coupling.

This was demonstrated in this chapter for oscillatory nets. However excitable and subexcitable nets with noise and variability are also robust under the influence of variability in the coupling. For values of Q and $\sigma_{v,q}$ similar to the values studied in this chapter no strong influences on the net dynamics can be found.

9 Summary and Outlook

In this thesis the influence of variability and noise on spatially extended systems is investigated in detail. The model systems are oscillatory and excitable nets of FitzHugh-Nagumo (FHN), Hodgkin-Huxley (HH) and reduced Hodgkin-Huxley elements, respectively.

It is shown that the interplay of additive variability and additive noise in an oscillatory net strongly influences the net dynamics. The additive variability induces pattern formation and even small values of the variability strength destroy the synchronised oscillation the net exhibits without variability. In a heterogeneous oscillatory net the synchronisation can be restored by additive noise. This noise-induced phase synchronisation exhibits a resonance-like dependency on the noise strength. The variability-induced pattern formation is also a resonance-like effect provided additive noise is present. In this case one finds maximal coherent patterns for intermediate values of the variability strength. To observe the variability-induced patterns the net has to exceed a certain size and thus the net size is important for the noise-induced synchronisation.

In contrast to the additive stochastic terms multiplicative variability can induce a transition to excitable and subexcitable dynamics in large and strongly coupled oscillatory nets. With additional multiplicative noise the borders of the described transitions depend on both the variability and the noise strength. Increasing the strengths of the multiplicative stochastic terms does thus lead to a suppression of the oscillatory net dynamics. For large variability and/or noise strengths the net rests in the variability and/or noise induced stable fixed point and no excitation is possible anymore. The transitions to excitable and subexcitable dynamics, which have a strong influence on the observed pattern formation, are explained by a systematic influence of the multiplicative stochastic terms on the system dynamics.

The Multiplicative variability has a similar influence on oscillatory nets as the multiplicative noise. Both lead to the same transitions and the observed patterns are alike. The additive variability and the additive noise do not affect the net dynamics in a similar way and their interplay leads to a new and unexpected phenomenon (noise-induced synchronisation).

Beyond oscillatory systems excitable and subexcitable nets are studied. It is shown that additive variability can induce pattern formation in such nets. The patterns are most coherent for intermediate variability strengths. This phenomenon can be called variability induced spatiotemporal stochastic resonance (STSR). It is furthermore demonstrated that the additive variability strongly influences the response of a subexcitable net of FHN elements to additive noise. Without variability one finds STSR with maximal coherent patterns for intermediate noise strengths. For a small variability strength the resonance curve is shifted to smaller values of the noise strength. For large values of the variability strength one does not find the STSR effect anymore.

The impact of the multiplicative variability on subexcitable nets of FHN elements is very different from the one of the additive variability. The multiplicative variability has a systematic influence on the net dynamics. It does not induce pattern formation, but causes a transition to excitable dynamics. Furthermore it is shown that the influence of

multiplicative variability and multiplicative noise on the net dynamics may not always be the same. Both induce a transition to excitable behaviour, but the multiplicative noise does additionally induce pattern formation.

A subexcitable net of FHN elements without noise can show coherent pattern formation in the presence of additive and multiplicative variability. For certain variability strengths one observes periodic excitation waves, which spread through the whole net. The waves are induced by the additive variability, and the ability of the net to support these waves is generated by the multiplicative variability. Hence the interplay of additive and multiplicative variability allows a complex deterministic net dynamics, where the pattern formation can neither be explained by the dynamics of the single elements of the net nor by the mean values of the model parameters.

These results demonstrate that the interplay of variability and noise may play an important role in spatially extended biological systems. It may be essential for pattern formation mechanisms, stochastic resonance effects and synchronisation. At least the additive variability may influence noise induced effects, such as temporal or spatiotemporal stochastic resonance.

The multiplicative stochastic terms have in addition a systematic influence on the system dynamics, which may cause a wide range of interesting phenomena, like variability and/or noise induced transitions between different regimes. These transitions can determine the pattern formation, which is found in a certain system. Furthermore the transition to excitable dynamics found in oscillatory nets may help to develop new strategies to suppress malfunction neural oscillations and to restore the functionality of neural networks.

The interplay of additive and multiplicative variability, for example in the parameters e and c of the FHN model, may be essential for the dynamics of a biophysical network, because it determines the net dynamics and allows for a coherent pattern formation. This is an interesting form of self-organisation of the net.

In a next step the influence of the correlation length of the variability on the dynamics of diffusively coupled FHN systems is investigated. It is demonstrated that an increasing correlation length of the additive variability can strongly reduce the strength of the additive variability, which is required to induce pattern formation in subexcitable nets. This makes it much more likely that additive variability might play a role for pattern formation in biological systems. Furthermore a large correlation length can strongly increase the mean life-time of excitation waves in subexcitable nets.

Studying the influence of the correlation length of multiplicative variability one finds completely different results. In this case increasing the correlation length disturbs the variability induced transitions. This implies that variability induced transitions in diffusively coupled nets can only be observed, if the correlation length of the variability is small compared to the other length scales of the system.

In general one can conclude that the correlation length of the variability may have a crucial influence on the dynamics of diffusively coupled biophysical networks. It might be particularly important for pattern forming processes.

Furthermore it is shown that variability in the coupling can induce coherent pattern formation in oscillatory nets of FHN elements. This pattern formation is only found if some elements are not (or barely) coupled to their neighbour elements anymore and oscillate freely. Finally the interplay of variability in the coupling and multiplicative variability is studied. The variability in the coupling is able to disturb the transition from oscillatory to excitable dynamics, which is caused by the multiplicative variability.

These results lead to the conclusion that variability in the coupling has an influence on the dynamics of spatially extended systems. However the strength of the variability in the coupling has to be very large to see such influences. For small values of the variability strength the dynamics of the observed nets are very robust under the influence of variability in the coupling.

The presented findings will contribute to the theoretical understanding of spatially extended systems influenced by variability and noise. However the research in this field is not completed yet and also in the course of this work topics have been explored that should be investigated further. It might, for example, be interesting to study multiplicative stochastic terms in other model parameters. Furthermore the interplay of variability and noise, which is correlated in time and/or space, is not studied yet. Beyond this the variability in the coupling should be examined in more detail. In this thesis variability in the coupling without a spatial correlation is chosen. Such a correlation might enhance the influence of the variability in the coupling on the net dynamics.

The interplay of variability and noise has been studied in a rather general framework using the paradigmatic FHN and HH systems. In a next step it would be interesting to study more realistic models to come closer to real biological systems. In this context it would be important to get experimental results. Perhaps this work does foster experimental research in the field of variability and/or noise induced pattern formation.

Bibliography

[1] S. Sawai, P. A. Thomason, and E. C. Cox. An autoregulatory circuit for long-range self-organization in dictyostelium cell populations. *Nature*, 433:323–326, 2004.

[2] A. N. Zaikin and A. M. Zhabotinsky. Concentration wave propagation in two-dimensional liquid-phase self-oscillating system. *Nature*, 225:535 – 537, 1970.

[3] P. Jung, A.H. Cornell-Bell, F. Moss, S. Kádár, J. Wang, and K. Showalter. Noise sustained waves in subexcitable media: From chemical waves to brain waves. *Chaos*, 8:567–575, 1998.

[4] A. M. Turing. The chemical basis of morphogenesis. *Phil. Trans. R. Soc.*, 237:37–72, 1952.

[5] A. Gierer and H. Meinhardt. A theory of biological pattern formation. *Kybernetik*, 12:30–39, 1972.

[6] M. C. Cross and P. C. Hohenberg. Pattern formation outside of equilibrium. *Rev. Mod. Phys.*, 65:851 – 1112, 1993.

[7] P. Jung and G. Mayer-Kress. Spatiotemporal stochastic resonace in excitable media. *Phys. Rev. Lett.*, 74:2130–2133, 1995.

[8] H. Busch and F. Kaiser. Influence of spatiotemporally correlated noise on structure formation in excitable media. *Phys. Rev. E*, 67:041105, 2003.

[9] A. S. Pikovsky and J. Kurths. Coherence resonance in a noise-driven excitable system. *Phys. Rev. Lett.*, 78:775–778, 1997.

[10] E. Ullner, A. Zaikin, J. García-Ojalvo, and J. Kurths. Noise-induced excitability in oscillatory media. *Phys. Rev. Lett.*, 91:180601, 2003.

[11] E. Glatt, H. Busch, A. Zaikin, and F. Kaiser. Noise-memory induced excitability and pattern formation in oscillatory neural models. *Phys. Rev. E*, 73:026216, 2006.

[12] J. Hasty, J. Pradines, M. Dolnik, and J. J. Collins. Noise-based switches and amplifiers for gene expression. *PNAS*, 97:2075–2080, 2000.

[13] J. García-Ojalvo and J. M. Sancho. *Noise in Spatially Extended Systems*. Springer, Berlin, 1999.

[14] F. Sagués, J. M. Sancho, and J. García-Ojalvo. Spatiotemporal order out of noise. *Rev. Mod. Phys.*, 79:829, 2007.

[15] J. Douglass, L. Wilkins, D. Pierson, E. Pantazelou, and F. Moss. Noise enhancement of information transfer in crayfish mechanoreceptors by stochastic resonance. *Nature*, 365:337–340, 1993.

[16] D. F. Russell, L. A. Wilkens, and F. Moss. Use of behavioural stochastic resonance by paddle fish for feeding. *Nature*, 402:291–294, 1999.

[17] J. T. Mettetal and A. van Oudenaarden. Necessary noise. *Science*, 317:463 – 464, 2007.

[18] A. T. Winfree. Biological rhythms and the behavior of populations of coupled oscillators. *J. Theor. Biol.*, 16:15–42, 1967.

[19] Y. Kuramoto. *Chemical oscillations, waves and turbulence.* Springer, Berlin, 1984.

[20] Y. Braiman, J. F. Lindner, and W. L. Ditto. Taming spatiotemporal chaos with disorder. *Nature*, 378:465–467, 1995.

[21] H. Chen and J. Zhang. Diversity-induced coherence resonance in spatially extended chaotic systems. *Phys. Rev. E*, 77:026207, 2008.

[22] M.-Th. Hütt, H. Busch, and F. Kaiser. The effect of biological variability on spatiotemporal patterns - model simulations for a network of biochemical oscillators. *Nova Acta Leopoldina NF 88*, 332:381–400, 2003.

[23] C. J. Tessone, C. R. Mirasso, R. Toral, and J. D. Gunton. Diversity-induced resonance. *Phys. Rev. Lett.*, 97:194101, 2006.

[24] M. Gassel, E. Glatt, and F. Kaiser. Doubly diversity-induced resonance. *Phys. Rev. E*, 76:016203, 2007.

[25] R. F. Schmidt, F. Lang, and G. Thews. *Physiologie des Menschen.* Springer, Berlin, 2005.

[26] J. Breckow and R. Greinert. *Biophysik: Eine Einführung.* Walter de Gruyter, Berlin, 1994.

[27] H. Beug, F. E. Katz, and G.Gerisch. Dictyostelium discoideum. *J. Cell Biol.*, 56:647–658, 1973.

[28] P. Bak, K. Chen, and C. Tang. A forest-fire model and some thoughts on turbulence. *Phys. Lett. A*, 147:297, 1990.

[29] B. Drossel and F. Schwabl. Self-organized critical forest-fire model. *Phys. Rev. Lett.*, 69:1629–1632, 1992.

[30] S. Alonso, I. Sendiña-Nadal, V. Pérez-Muñuzuri, J. M. Sancho, and F. Sagués. Regular wave propagation out of noise in chemical active media. *Phys. Rev. Lett.*, 87:078302, 2001.

[31] A. L. Hodgkin and A. F. Huxley. A quantitative description of membrane current and its application to conduction and excitation in nerve. *J. Physiol.*, 117:500–544, 1952.

[32] K. F. Bonhoeffer. Activation of passive iron as a model for the excitation of nerve. *J. Gen. Physiol.*, 32:69–91, 1948.

[33] R. A. FitzHugh. Impulse and physiological states in theoretical models of nerve membranes. *Biophys J.*, 1:445, 1961.

[34] J. S. Nagumo and S. Yoshizawa. An active pulse transmission line simulating nerve axon. *Proc. Inst. Radio Engineers*, 50:2061, 1962.

[35] J. García-Ojalvo, M. B. Elowitz, and S. H. Strogatz. Modeling a synthetic multicellular clock: Repressilators coupled by quorum sensing. *PNAS*, 101:10955–10960, 2004.

[36] J. Keener and J. Sneyd. *Mathematical Physiology.* Springer, Berlin, 1998.

[37] L. Gammaitoni, P. Hänggi, P. Jung, and F. Marchesoni. Stochastic resonance. *Rev. Mod. Phys.*, 70:223–288, 1998.

[38] E. Glatt, M. Gassel, and F. Kaiser. Variability induced transition in a net of neural elements: From oscillatory to excitable behavior. *Phys. Rev. E*, 73:066230, 2006.

[39] E. Glatt, M. Gassel, and F. Kaiser. Variability sustained pattern formation in subexcitable media. *Phys. Rev. E*, 75:026206, 2007.

[40] E. Glatt, M. Gassel, and F. Kaiser. Noise-induced synchronisation in heterogeneous nets of neural elements. *Europhys. Lett.*, 81:40004, 2008.

[41] A. Neiman, L. Schimansky-Geier, A. Cornell-Bell, and F. Moss. Noise-enhanced phase synchronization in excitable media. *Phys. Rev. Lett.*, 83:004896, 1999.

[42] H. Kitajima and J. Kurths. Synchronized firing of FitzHugh-Nagumo neurons by noise. *Chaos*, 15:023704, 2005.

[43] G. V. Osipov, J. Kurths, and C. Zhou. *Synchronization in Oscillatory Networks.* Springer, Berlin, 2007.

[44] J. Kurths and C. Zhou. Noise, synchronization and coherence in chaotic oscillators. *International Journal of Modern Physics B*, 17:4023–4044, 2003.

[45] A. Pikovsky, M. Rosenblum, and J. Kurths. *Synchronization. A Universal Concept in Nonlinear Sciences.* Cambridge University Press, Cambridge, 2001.

[46] V. Pérez-Muñuzuri, F. Sagués, and J. M. Sancho. Lifetime enhancement of scroll rings by spatiotemporal fluctuations. *Phys. Rev. E.*, 62:94, 2000.

[47] S. Alonso, J. M. Sancho, and F. Saguès. Suppression of scroll wave turbulence by noise. *Phys. Rev. E.*, 70:067201, 2004.

[48] S. Mangioni, R. Deza, H. Wio, and R. Toral. Disordering effects of color in nonequilibrium phase transitions induced by multiplicative noise. *Phys. Rev. Lett.*, 79:2389, 1997.

[49] S. Mangioni, R. Deza, H. Wio, and R. Toral. Nonequilibrium phase transitions induced by multiplicative noise: Effects of self-correlation. *Phys. Rev. E*, 61:223, 2000.

[50] J. M. Sancho, M. S. Miguel, S. L. Katz, and J. D. Gunton. Analytical and numerical studies of multiplicative noise. *Phys. Rev. A*, 26:1589, 1981.

[51] M. Matsumoto and T. Nishimura. Mersenne twister: A 623-dimensionally equidistributed uniform pseudo-random number generator. *ACM Transactions on Modeling and Computer Simulation*, 8:3–30, 1998.

[52] S. De Monte, F. d'Ovidio, and E. Mosekilde. Coherent regimes of globally coupled dynamical systems. *Phys. Rev. Lett.*, 90:054102, 2003.

[53] I. Gomes Da Silva, S. De Monte, F. d'Ovidio, R. Toral, and C. R. Mirasso. Coherent regimes of mutually coupled Chua's circuits. *Phys. Rev. E*, 73:036203, 2006.

[54] D. B. Murray, M. Beckmann, and H. Kitano. Regulation of yeast oscillatory dynamics. *PNAS*, 104:2241–2246, 2007.

[55] M. R. Roussel and D. Lloyd. Observation of a chaotic multioscillatory metabolic attractor by real-time monitoring of a yeast continuous culture. *FEBS J.*, 274:1011–1018, 2007.

[56] C. H. Johnson, S. S. Golden, M. Ishiura, and T. Kondo. Circadian clocks in prokaryotes. *Molecular Microbiology*, 21:5–11, 1996.

[57] L. Becks, F. M. Hilker, H. Malchow, K. Jürgens, and H. Arndt. Experimental demonstration of chaos in a microbial food web. *Nature*, 435:1226–1229, 2005.

[58] P. A. Tass. *Phase Resetting in Medicine and Biology. Stochastic Modelling and Data Analysis.* Springer, Berlin, 1999.

[59] A. L. Benabid, P. Pollack, and C. Gervason. Long-term suppression of tremor by chronic stimulation of the ventral intermediate thalamic nucleus. *Lancet*, 337:403–406, 1991.

[60] M. G. Rosenblum and A. S. Pikovsky. Controlling synchronization in an ensemble of globally coupled oscillators. *Phys. Rev. Lett.*, 92:114102, 2004.

[61] M. Gassel, E. Glatt, and F. Kaiser. Time-delayed feedback in a net of neural elements: Transition from oscillatory to excitable dynamics. *Fluct. and Noise Lett.*, 7(3):225, 2007.

[62] S. Kádár, J. Wangi, and K. Showalter. Noise-supported travelling waves in subexcitable media. *Nature*, 391:770 – 772, 1998.

[63] S. Alonso, I. Sendina-Nadal, V. Perez-Munuzuri, J. M. Sancho, and F. Sagues. Regular wave propagation out of noise in chemical active media. *Phys. Rev. Lett.*, 87:078302, 2001.

[64] C. Zhou J. Kurths and B. Hu. Array-enhanced coherence resonance: Nontrivial effects of heterogeneity and spatial independence of noise. *Phys. Rev. Lett.*, 87:098101, 2001.

[65] E. Glatt, M. Gassel, and F. Kaiser. Pattern formation in subexcitable media: Interplay of noise and variability. *Proceedings of SPIE*, 6602:66021F, 2007.

[66] J. J. Collins, C. C. Chow, A. C. Capela, and T. T. Imhoff. Aperiodic stochastic resonance. *Phys. Rev. E*, 54:5575 – 5584, 1996.

[67] S.-G. Lee, A. Neiman, and S. Kim. Coherence resonance in a Hodgkin-Huxley neuron. *Phys. Rev. E*, 57:3292 – 3297, 1997.

[68] Y. Wang, D. T. Chik, and Z. D. Wang. Coherence resonance and noise -induced synchronization in globally coupled Hodgkin-Huxley neurons. *Phys. Rev. E*, 61:740, 2000.

[69] B. Drossel. Random boolean networks. *Review of Nonlinear Dynamics and Complexity*, 1, 2007.

[70] R. Albert and A.-L. Barabási. Statistical mechanics of complex networks. *Reviews of Modern Physics*, 74:47, 2002.

[71] C. Marr, M. Müller-Linow, and M.-T. Hütt. Regularizing capacity of metabolic networks. *Phys. Rev. E*, 75:041917, 2007.

[72] S. Weber, M.-Th. Hütt, and M. Porto. Pattern formation and efficiency of reaction-diffusion processes on complex networks. *EPL*, in print, 2008.

[73] M. Müller-Linow, C. Marr, and M.-T. Hütt. Topology regulates the distribution pattern of excitations in excitable dynamics on graphs. *Phys. Rev. E*, 74:016112, 2006.

Zusammenfassung

In dieser Doktorarbeit wird der Einfluss von Variabilität und Rauschen auf räumlich ausgedehnte Systeme im Detail studiert. Die Modellsysteme sind oszillatorische und exzitatorische Netze, bestehend aus FitzHugh-Nagumo (FHN), Hodgkin-Huxley (HH) beziehungsweise reduzierten Hodgkin-Huxley Elementen.

Es wird gezeigt, dass das Zusammenspiel von additiver Variabilität und additivem Rauschen die Systemdynamik eines oszillatorischen Netzes stark beeinflusst. Die additive Variabilität induziert Strukturbildung und daher zerstören schon kleine Werte der Variabilitätsstärke die synchrone Oszillation, welche das Netz ohne Variabilität zeigt. In einem heterogenen oszillatorischen Netz kann die Synchronisation durch additives Rauschen wieder hergestellt werden. Diese rauschinduzierte Phasensynchronisation zeigt eine resonanzartige Abhängigkeit von der Rauschstärke. Die variabilitätsinduzierte Strukturbildung ist auch ein resonanzartiger Effekt, vorausgesetzt additives Rauschen ist vorhanden. In diesem Fall findet man Strukturen mit maximaler Kohärenz für mittlere Werte der Variabilitätsstärke. Die variabilitätsinduzierten Strukturen können nur in ausreichend großen Netzen beobachtet werden und daher spielt die Netzgröße eine wichtige Rolle für die rauschinduzierte Synchronisation.

Im Gegensatz zu den additiven stochastischen Termen kann multiplikative Variabilität einen Übergang zu exzitatorischer und subexzitatorischer Dynamik in großen und stark gekoppelten oszillatorischen Netzen induzieren. In Netzen mit zusätzlichem multiplikativem Rauschen hängen die Grenzen der beschriebenen Übergänge von der Rausch- und der Variabilitätsstärke ab. Eine Erhöhung der Stärke der multiplikativen stochastischen Terme führt somit zu einer Unterdrückung der oszillatorischen Netzdynamik. Für große Variabilitäts- bzw. Rauschstärken ruht das Netz im variabilitäts- bzw. rauschinduzierten stabilen Fixpunkt und eine Anregung ist nicht mehr möglich. Die Übergänge zu exzitatorischer und subexzitatorischer Dynamik, welche einen starken Einfluss auf die beobachtbare Strukturbildung haben, können mit einem systematischen Einfluss der multiplikativen stochastischen Terme auf die Systemdynamik erklärt werden.

Die multiplikative Variabilität hat einen ähnlichen Einfluss auf oszillatorische Netze wie das multiplikative Rauschen. Beide führen zu den gleichen Übergängen und die zu beobachteten Strukturen sind sich dabei sehr ähnlich. Die additive Variabilität und das additive Rauschen beeinflussen die Netzdynamik nicht auf eine ähnliche Art und Weise und ihr Zusammenspiel führt zu einem neuen und unerwarteten Phänomen (rauschinduzierte Synchronisation).

Neben oszillatorischen Systemen werden auch exzitatorische und subexzitatorische Netze untersucht. Es wird gezeigt, dass additive Variabilität in solchen Netzen Strukturbildung anregen kann. Die Strukturen sind dabei am kohärentesten für mittlere Werte der Variabilitätsstärke. Dieses Phänomen kann man als variabilitätsinduzierte raumzeitliche stochastische Resonanz (STSR) bezeichnen. Es wird weiterhin gezeigt, dass die additive Variabilität die Antwort eines subexzitatorischen Netzes (bestehend aus FHN Elementen) auf additives Rauschen stark beeinflusst. Ohne Variabilität findet man STSR mit maximal kohärenten Strukturen für mittlere Rauschstärken. Für eine kleine Variabilitätsstärke ist

die Resonanzkurve zu kleineren Werten der Rauschstärke verschoben. Für große Werte der Variabilitätsstärke findet man den STSR-Effekt nicht mehr.

Die Wirkung der multiplikativen Variabilität auf subexzitatorische FHN Systeme unterscheidet sich sehr von der der additiven Variabilität. Die multiplikative Variabilität hat einen systematischen Einfluss auf die Dynamik. Sie induziert keine Strukturbildung, bewirkt aber einen Übergang zu exzitatorischer Dynamik. Darüber hinaus wird gezeigt, dass der Einfluss von multiplikativem Rauschen und multiplikativer Variabilität auf die Netzdynamik nicht immer gleich ist. Beide induzieren einen Übergang zu exzitatorischem Verhalten, aber das multiplikative Rauschen führt zusätzlich noch zu Strukturbildung.

Ein subexzitatorisches Netz ohne Rauschen, bestehend aus FHN Elementen, kann unter dem Einfluss von additiver und multiplikativer Variabilität kohärente Strukturen hervorbringen. Für bestimmte Werte der Variabilitätsstärke beobachtet man periodische Anregungswellen, welche durch das ganze Netz laufen. Diese Wellen werden von der additiven Variabilität angeregt und die multiplikative Variabilität unterstützt die Wellenausbreitung. Auf diese Art und Weise ermöglicht das Zusammenspiel von additiver und multiplikativer Variabilität eine komplexe deterministische Netzdynamik, wobei die Strukturbildung weder durch die Dynamik der Einzelelemente des Netzes noch durch die Mittelwerte der Modellparameter erklärt werden kann.

Diese Ergebnisse zeigen, dass das Zusammenspiel von Variabilität und Rauschen eine wichtige Rolle in räumlich ausgedehnten biologischen Systemen spielen kann. Es könnte für Strukturbildungsprozesse, stochastische Resonanz und Synchronisation wesentlich sein. Zumindest kann die additive Variabilität rauschinduzierte Effekte, wie zeitliche oder raumzeitliche stochastische Resonanz, beeinflussen.

Die multiplikativen stochastischen Terme haben zusätzlich einen systematischen Einfluss auf die Systemdynamik, welcher eine Reihe von interessanten Phänomen, wie variabilitäts- bzw. rauschinduzierte Übergänge zwischen unterschiedlichen Regimen, verursachen kann. Diese Übergänge bestimmen die Strukturbildung, welche in einem bestimmten System beobachtet werden kann. Darüber hinaus könnte der in oszillatorischen Netzen gefundene Übergang zu exzitatorischer Dynamik helfen, neue Strategien zur Unterdrückung ungewollter neuronaler Oszillationen zu entwickeln und die Funktionalität neuronaler Netzwerke wieder herzustellen.

Das Zusammenspiel von additiver und multiplikativer Variabilität, zum Beispiel in den Parametern e und c des FHN Modells, könnte wesentlich für die Dynamik eines biophysikalischen Netzwerkes sein, da es die Netzdynamik bestimmt und kohärente Strukturbildung ermöglicht. Dies ist eine interessante Form der Selbstorganisation des Netzes.

Als nächstes wird der Einfluss der Korrelationslänge der Variabilität auf die Dynamik diffusiv gekoppelter FHN Systeme untersucht. Es wird gezeigt, dass eine zunehmende Korrelationslänge der additiven Variabilität die Variabilitätsstärke, welche erforderlich ist um Muster in subexzitatorischen Netzen zu erzeugen, deutlich reduzieren kann. Dies macht es wahrscheinlicher, dass additive Variabilität eine wichtige Rolle bei Strukturbildungsprozessen in biologischen Systeme spielt. Darüber hinaus kann eine große Korrelationslänge die mittlere Lebenszeit von Anregungswellen in subexzitatorischen Netzen deutlich verlängern.

Untersucht man den Einfluss der Korrelationslänge bei multiplikativer Variabilität findet man komplett andere Ergebnisse. In diesem Fall stört eine zunehmende Korrelationslänge die variabilitätsinduzierten Übergänge. Dies impliziert, dass variabilitätsinduzierte Übergänge in diffusiv gekoppelten Netzen nur beobachtet werden können, wenn die Korrelationslänge der Variabilität im Vergleich mit den anderen Längenskalen des

Systems klein ist.

Allgemein kann man folgern, dass die Korrelationslänge der Variabilität einen großen Einfluss auf die Dynamik von diffusiv gekoppelten biophysikalischen Netzwerken habt. Besonders wichtig könnte die Korrelationslänge für Strukturbildungsprozesse sein.

Weiterhin wird gezeigt, dass Variabilität in der Kopplung kohärente Strukturbildung in oszillatorischen Netzen, bestehend aus FHN Elementen, induzieren kann. Diese Strukturbildung kann nur beobachtet werden, wenn einige Elemente nicht mehr oder kaum noch an ihre Nachbarelemente gekoppelt sind und somit frei oszillieren. Darüber hinaus wird das Zusammenspiel von Variabilität in der Kopplung und multiplikativer Variabilität untersucht. Die Variabilität in der Kopplung ist in der Lage den Übergang von oszillatorischer zu exzitatorischer Dynamik, welcher durch die multiplikative Variabilität induziert wird, zu stören.

Diese Ergebnisse führen zu der Schlussfolgerung, dass Variabilität in der Kopplung einen Einfluss auf die Dynamik räumlich ausgedehnter Systeme mit diffusiver Kopplung hat. Allerdings muss die Stärke der Variabilität in der Kopplung sehr groß sein, um solche Einflüsse zu beobachten. Für kleine Werte der Variabilitätsstärke sind die Dynamiken der untersuchten Netze sehr robust unter dem Einfluss von Variabilität in der Kopplung.

Die vorgelegten Ergebnisse tragen zum theoretischen Verständnis von räumlich ausgedehnten Systemen unter dem Einfluss von Variabilität und Rauschen bei. Allerdings ist die Forschung auf diesem Gebiet noch lange nicht abgeschlossen und auch im Verlauf dieser Doktorarbeit sind Themen untersucht worden, welche noch weiterführend erforscht werden sollten. Es könnte zum Beispiel interessant sein multiplikative stochastische Terme auch in anderen Modellparametern zu untersuchen. Außerdem wurde das Zusammenspiel von Variabilität und Rauschen mit zeitlicher und/oder räumlicher Korrelation noch nicht erforscht. Darüber hinaus sollte die Variabilität in der Kopplung noch genauer untersucht werden. In dieser Arbeit wurde Variabilität in der Kopplung ohne räumliche Korrelation gewählt. Solch eine Korrelation könnte den Einfluss der Variabilität in der Kopplung auf die Netzdynamik verstärken.

Das Zusammenspiel von Variabilität und Rauschen wurde in einem eher allgemeinen Rahmen unter Benutzung der beispielhaften FHN und HH Systeme untersucht. Weiterführend wäre es interessant realistischere Modelle, welche stärker an reale biologische Systeme angelehnt sind, zu untersuchen. In diesem Zusammenhang wäre es wichtig experimentelle Ergebnisse zu erhalten. Vielleicht regt diese Arbeit zu experimenteller Forschung auf dem Gebiet der variabilitäts- bzw. rauschinduzierten Musterbildung an.

Danksagung

Viele Personen haben mich während der Entstehung dieser Arbeit unterstützt und einigen möchte ich hier explizit danken:

- Herrn Prof. Friedemann Kaiser möchte ich dafür danken, dass er mir ermöglicht hat in seiner Arbeitsgruppe zu promovieren. Von seiner umfassenden Erfahrung auf dem Gebiet der nichtlinearen Dynamik und von den Diskussionen in der Arbeitsgruppe habe ich sehr profitiert.

- Weiterhin möchte ich mich bei den aktuellen und ehemaligen Mitgliedern der Arbeitsgruppe Martin Gassel, Kristian Motzek und Tobias Richter für den ungezwungenen Umgang, die freundschaftliche Atmosphäre in der Arbeitsgruppe und die vielen Diskussionen bedanken. Besonderer Dank gilt dabei Martin Gassel für die direkte wissenschaftliche Zusammenarbeit und Tobias Richter dafür, dass er mich freundschaftlich durch die Höhen und Tiefen der Promotion begleitet hat.

- Prof. M.-Th. Hütt möchte ich für die wissenschaftlichen Diskussionen zu Beginn meiner Promotion danken.

- Weiterhin möchte ich mich bei Prof. Dr. Felicitas Pfeifer und Monika Medina, den Mitarbeiten des Graduiertenkolleg 340, für ihre Unterstützung bedanken. Als Stipendiat des Graduiertenkollegs war es mir möglich einen Einblick in das große Gebiet der Biologie zu erhalten, dabei war der freundliche und ungezwungen Umgang mit den übrigen Mitgliedern des Graduiertenkollegs eine große Hilfe.

- Meiner Freundin Ilona Türschmann danke ich dafür, dass ich auch mal nicht an Physik gedacht habe.

- Besonderer Dank gilt natürlich auch meinen Eltern und meiner Schwester die mich stets unterstützt und ohne deren Hilfe diese Arbeit wohl nie entstanden wäre.

Curriculum Vitae

Persönliche Daten

Name	Erik Glatt
Geburtstag	16. September 1978
Geburtsort	Mannheim
Nationalität	deutsch
Anschrift	Heinrichstr. 111, 64283 Darmstadt

Schulbildung

1985 bis 1989	Wingertsbergschule Lorsch
1989 bis 1998	Starkenburggymnasium Heppenheim
06/1998	Abitur, Gesamtnote: 1,6

Zivildienst

08/1998 bis 09/1999	Chirurgisch-Orthopädische Fachklinik Lorsch

Hochschulausbildung

10/1999 bis 03/2005	Studium der Physik an der Technischen Hochschule Darmstadt
10/2001 bis 10/2002	EU-SOCRATES Austauschjahr am Trinity College, Dublin
01/2004 bis 01/2005	Diplomarbeit am Institut für Angewandte Physik, Technischen Hochschule Darmstadt Betreuer: Prof. Dr. F. Kaiser und H. Busch
03/2005	Physik-Diplom, Gesamtnote: sehr gut
04/2005 bis 2008	Promotion am Institut für Angewandte Physik, Technischen Hochschule Darmstadt Betreuer: Prof. Dr. F. Kaiser

Sonstiges

2004 bis 2005	Tutor in den Übungen zu den Vorlesungen in theoretischer Physik: *Vorbereitung auf die Quantenmechanik*, *Quantenmechanik* und *Statistische Physik*
2004 bis 2005	Betreuung einer Diplomarbeit
2005 bis 2008	Betreuung von Vorträgen im Seminar „*Komplexe Systeme: Nichtlineare Prozesse, Fluktuationen und Strukturbildung*“

Hiermit erkläre ich an Eides Statt, dass ich
die vorliegende Dissertation selbständig verfasst
und nur die angegebenen Hilfsmittel verwendet habe.
Ich habe bisher keinen Versuch unternommen, an einer
anderen Hochschule das Promotionsverfahren einzuleiten.

Darmstadt, 25.6.2008

(Erik Glatt)